NASA TECHNICAL MEMORANDUM

NASA TM X-2086

NASA TM X-2086

PERFORMANCE OF A 10° CONICAL PLUG NOZZLE WITH VARIOUS PRIMARY FLAP AND NACELLE CONFIGURATIONS AT MACH NUMBERS FROM 0 TO 1.97

by Douglas E. Harrington

Lewis Research Center
Cleveland, Ohio 44135

NATIONAL AERONAUTICS AND SPACE ADMINISTRATION • WASHINGTON, D. C. • DECEMBER 1970

1. Report No. NASA TM X-2086	2. Government Accession No.	3. Recipient's Catalog No.
4. Title and Subtitle PERFORMANCE OF A 10° CONICAL PLUG NOZZLE WITH VARIOUS PRIMARY FLAP AND NACELLE CONFIGURATIONS AT MACH NUMBERS FROM 0 TO 1.97		5. Report Date December 1970 6. Performing Organization Code
7. Author(s) Douglas E. Harrington		8. Performing Organization Report No. E-5698 10. Work Unit No. 720-03
9. Performing Organization Name and Address Lewis Research Center National Aeronautics and Space Administration Cleveland, Ohio 44135		11. Contract or Grant No. 13. Type of Report and Period Covered Technical Memorandum
12. Sponsoring Agency Name and Address National Aeronautics and Space Administration Washington, D.C. 20546		14. Sponsoring Agency Code
15. Supplementary Notes		

16. Abstract

A plug nozzle with a ratio of throat area to nacelle area of 0.23 was tested with a full-length plug and several truncated plugs and at several secondary flow ratios. Internal expansion was varied by translation of a cylindrical secondary shroud. A nozzle gross thrust coefficient of 1.02 was obtained at Mach 1.97 at a supersonic cruise pressure ratio of 27 with a secondary weight-flow ratio of 4 percent. At subsonic cruise, nozzle gross thrust coefficient was sensitive to the design of the nacelle and primary nozzle flap.

17. Key Words (Suggested by Author(s))	18. Distribution Statement
Plug nozzle Air breathing propulsion Turbojet engines Exhaust nozzles	Unclassified - unlimited

19. Security Classif. (of this report)	20. Security Classif. (of this page)	21. No. of Pages	22. Price*
Unclassified	Unclassified	49	$3.00

*For sale by the National Technical Information Service, Springfield, Virginia 22151

PERFORMANCE OF A 10° CONICAL PLUG NOZZLE WITH VARIOUS PRIMARY FLAP AND NACELLE CONFIGURATIONS AT MACH NUMBERS FROM 0 TO 1.97

by Douglas E. Harrington

Lewis Research Center

SUMMARY

An experimental investigation was conducted in the Lewis 8- by 6-Foot Supersonic Wind Tunnel to determine the performance characteristics of several 10° half-angle conical plug nozzles. Comparisons were made between three nozzles with various primary flap and nacelle configurations to determine the effect of these geometric variables on performance. Internal expansion was varied by translation of a cylindrical secondary shroud. Secondary flow was varied from approximately 0 to 10 percent of primary weight flow. Truncated plug configurations were tested with and without base flow.

At supersonic cruise a nozzle gross thrust coefficient of 1.02 was obtained at Mach 1.97 at a pressure ratio of 27 and a corrected secondary weight-flow ratio of 4 percent with a 17° conical primary flap, a full-length plug, and an extended secondary shroud. Truncation of the plug had no appreciable effect on gross thrust coefficient.

At subsonic cruise, nozzle gross thrust coefficient was sensitive to the geometry of the nacelle and the primary nozzle flap. For subsonic cruise at a pressure ratio of 2.8, a corrected secondary weight-flow ratio of 4 percent, and a Mach number of 0.85, truncation of the plug to 50 percent of full length reduced nozzle gross thrust coefficient from 0.91 to 0.90.

Takeoff nozzle gross thrust coefficients ranged from approximately 0.97 to 0.98 at a pressure ratio of 3.0 and a corrected secondary weight-flow ratio of 0.04. Pumping characteristics at takeoff were sensitive to the location of the shroud. As expected, there was no pumping with a fully retracted shroud. Extending the shroud to 18 percent of the plug length, however, provided some cooling flow with little effect on performance.

INTRODUCTION

Supersonic cruise aircraft, which operate over a wide range of flight and engine conditions, require variable geometry exhaust nozzles to maintain efficient operation at off-design conditions. In addition to maintaining high performance, the complexity of the exhaust nozzle system should be kept to a minimum. A nozzle that has the potential of meeting these requirements is the plug nozzle. Isentropic plug nozzles have high performance when operated under static conditions. However, when operated with external flow, the performance of these nozzles is adversely affected at off-design conditions, as reported in references 1 to 3. This decrement in performance results from the steep primary flap boattail angles inherent in this concept. With external flow, low pressures exist on this boattail, and the nozzle flow expands to the local pressure at the trailing edge of the boattail rather than to free-stream ambient pressure. This results in boattail drag and overexpansion losses on the plug surface. A compromise in design may be made by using a low-angle conical plug rather than an isentropic plug. The boattail angles are reduced and the problems of overexpansion and boattail drag are partially alleviated. A secondary shroud is frequently used with this concept to provide internal expansion at high pressure ratios.

Tests have been conducted, references 4 to 11, to optimize the performance of the low-angle conical plug nozzle. These investigations have studied the effect of plug truncation, secondary flow, secondary shroud geometry and location, and plug apex angle on nozzle performance. In addition, various methods of varying primary throat area have been investigated.

At transonic speeds nozzle performance is particularly sensitive to external flow effects. These effects are dependent on the manner in which the nozzle is installed on the airframe. To investigate this installation effect for the F-106 podded engine configuration described in reference 12, a series of nozzle concepts are being flight tested and the results compared to those obtained in wind tunnel tests of the nozzle as an isolated component.

This report presents the performance characteristics of an isolated conical plug nozzle which subsequently was flight tested. This nozzle was mounted on a cylindrical jet-exit model in the Lewis 8- by 6-Foot Supersonic Wind Tunnel. Testing was conducted over a range of Mach numbers from 0 to 1.97. Variations were made in the primary flap and nacelle geometries to determine the effect on nozzle performance. In addition, the effect of plug truncation on performance was also evaluated. Secondary flow was varied from approximately 0 to 10 percent of primary weight flow. Internal expansion was varied by translating a cylindrical secondary shroud.

APPARATUS AND PROCEDURE

Installation

The jet exit model was strut mounted in the test section of the Lewis 8- by 6-Foot Supersonic Wind Tunnel as shown in figure 1. The geometry of the model and its thrust-measuring system are shown in figure 2. The main part of the model was a strut-supported cylinder with a closed nose. The model external shell was grounded and supported from the tunnel ceiling by a hollow, vertical strut. The adapter portion of the model was attached to the air bottle, which was cantilevered by flow tubes from supply manifolds located outside the test section. Front and rear bearings supported the air bottle. Thus, the axial force acting on the floating part of the model, including both the adapter and nozzle sections, was transmitted to the load cell, located in the nose of the model shell.

To obtain the nozzle performance presented herein, the friction drag on the floating portion of the model designated as the adapter section was estimated and added to the force measured by the load cell. The downstream end of the adapter section was arbitrarily selected as being 0.75 model diameter upstream of the nozzle throat (x_c/l_c = -0.386). (Symbols are defined in appendix A.) Friction drag on the adapter section was estimated using the semiempirical, flat-plate, local skin-friction coefficient (given in fig. 6 of ref. 13) as a function of free-stream Mach number and Reynolds number. The coefficient accounts for variations in boundary-layer thickness and flow profile with Reynolds number. Previous measurements of the boundary-layer characteristics at the aft end of this jet exit model (ref. 14) indicated that the profile and thickness were essentially the same as that computed for a flat-plate of equal length. The average ratio of boundary-layer momentum thickness to model diameter was approximately 0.02. The strut wake appeared to affect only a localized region near the top of the model and resulted in a lower local free-stream velocity than measured on the side and bottom of the model. Therefore, the results of reference 13 were used without correction for three-dimensional flow effects or strut interference effects. The calculated friction drag of the adapter section was added to the load cell reading to obtain the thrust-minus-drag of the nozzle section.

A static calibration of the thrust-measuring system was obtained by applying a known force to the nozzle and measuring the output of the load cell. To minimize changes in the calibration due to variations in temperature (e.g., aerodynamic heating due to external flow), the load cell was surrounded by a water-cooled jacket and was maintained at a constant temperature.

Primary and secondary air were provided by means of airflow supply lines which entered the model through the support strut and are shown schematically in figure 2. Secondary air in the central air bottle passed through crossover struts inside the model

to simulate cooling flow for the primary nozzle flap and the internal surface of the secondary shroud. With the plug truncated, a small portion of the secondary flow was allowed to pass through the hollow plug support struts to provide plug base bleed. A uniform primary flow was maintained by using two choke plates and an airflow straightener upstream of station 7.

Primary and secondary weight-flow rates were determined from standard ASME flow-metering orifices located in the air supply lines. The ambient pressure was constant for a given free-stream Mach number; thus, a variation in nozzle pressure ratio was obtained by varying the nozzle total pressure P_7.

Nozzle Geometry

The various plug nozzle configurations that were tested are shown in figure 3. Each of the nozzles had a 10° half-angle conical plug and differed mainly in primary flap and nacelle afterbody geometry. Two conical primary flaps were tested with boattail angles of 17° and 14°. The geometrical details are shown in figure 3(a). A translating secondary shroud was simulated by using four cylindrical shroud lengths. The 17° conical primary flap was tested with the secondary shroud in all four positions while the 14° conical primary was tested only with the shroud completely retracted ($x_c/l_c = -0.116$). These nozzles had an overall design pressure ratio of 36.6. In addition, a rounded primary flap with a 14° trailing-edge angle was tested and is shown in figure 3(b). A four-position secondary shroud was again used. The design pressure ratio of this nozzle was reduced to 27.86. Since the nozzle throat area was fixed, it was necessary to boattail the nacelle so that the proper shroud diameter was obtained for this lower design pressure ratio. Shroud variables for the various nozzles are listed in table I.

In addition to testing a full-length plug, the 17° conical primary was tested with two truncated plugs which are shown in figure 3(c). One was 75 percent of full length while the other was 50 percent of full length. The full length of the plug is defined as the distance between the nozzle throat and the plug tip. The throat was assumed to be normal to the plug surface at the primary lip. For the 75-percent plug a small portion of the secondary flow was allowed to flow through each of the three hollow support struts to the open plug base to provide base bleed. The 50-percent plug was tested both with an open and a closed plug base.

The 17° conical primary was also tested with a flare on the nacelle to simulate a larger nacelle diameter. This flare, shown in figure 3(d), had a tapered forward-facing surface and a tapered rearward-facing surface. The nozzle gross thrust coefficient presented for this configuration does not include the force on the forward-facing surface. This force was determined from a pressure integration and added to the nozzle thrust-

TABLE I. - SHROUD VARIABLES

[Nozzle throat to nacelle area ratio, A_8/A_m, 0.23; secondary air to nozzle throat area ratio, A_s/A_8, 0.40.]

Type of primary	Overall design pressure ratio	Shroud length to plug length ratio, x/l	Internal area ratio, A_9/A_8
14^o or 17^o conical	36.60	-0.116	[a]1.0
		-.076	[a]1.0
		.223	[b]2.94
		.347	[b]3.30
14^o rounded	27.86	-0.167	[a]1.0
		.011	[a]1.0
		.182	[b]2.74
		.366	[b]3.04

[a]For these configurations A_9 becomes A_8.

[b]A_9 is the flow area between external shroud and plug surface (see fig. 3).

minus-drag determined from the load cell. The flared nacelle was tested only at one shroud location, $x_c/l_c = -0.087$.

Instrumentation

Details of temperature and pressure instrumentation at station 7 are shown in figure 4(a). Pressures in the primary airflow passage were measured by two static-pressure orifices and a total-pressure rake containing 11 tubes. Primary nozzle total pressure was obtained from an integrated average of these pressures. The accompanying table lists pressure orifice spacing as distance y from the inner surface of the passage. Primary- and secondary-air total temperatures were measured by copper-constantan thermocouples. Secondary-air total-pressure instrumentation is shown in figure 4(b). Secondary-air total pressure was assumed to be the average of four pressures recorded by tubes located at 60^o, 165^o, 195^o, and 300^o, circumferentially.

Plug surface static-pressure orifices were located at 180^o circumferentially and are shown in figure 4(c). The plug was divided into three segments. The static-pressure orifices for each segment were located at the centroids of equal projected areas. Thus, the force on each segment of the plug was determined by pressure-area integration. Orifice 1 was not included in the area weighting of the plug but was used to determine the nozzle throat pressure for the conical primaries. For the conical prima-

ries, total plug force was obtained by summing the forces of the three segments of the plug. Plug surface force for the 75-percent plug was determined by adding the forces on segments 1 and 2, while plug surface force for the 50-percent plug was determined by the force on segment 1. For the 14° rounded primary, plug force was obtained by summing the force downstream of the throat station ($x_r = 0$) on the first segment with the forces of the remaining two segments. No attempt was made to determine plug skin-friction drag. The accompanying table presents the axial location of each orifice relative to the nozzle throat station for the conical primaries ($x_c = 0$).

Plug-base static-pressure locations for the truncated plugs (open base) are shown in figure 4(d). Plug base force was then determined by averaging the four base statics and assuming this average base pressure acted on the entire base area. For the configuration with the 50-percent plug (closed base) the location of the plug-base static pressures is shown in figure 4(e). The pressure orifices were situated at the centroids of equal area. The base force was then determined by pressure-area integration. Primary flap static-pressure instrumentation is shown in figure 4(f). The conical primary boattails each had four static-pressure orifices located at the centroids of equal projected areas. The primary boattail drag was then determined from pressure-area integration of these four pressures. The force on the 14° rounded primary was obtained by using two static-pressure orifices and included only the force on the portion of the surface downstream of the secondary shroud. Static-pressure instrumentation for the flared nacelle is shown in figure 4(g). Four pressures were used to determine the force on the forward-facing surface. This force was then added to the thrust-minus-drag determined from the load cell. The force on the rearward-facing surface was also determined from four pressures.

RESULTS AND DISCUSSION

In this report, comparisons will be made between the various nozzles tested to determine the effect of several geometric variables on nozzle performance characteristics. In order to facilitate this comparison, a nozzle pressure ratio schedule was assumed for a typical turbojet engine designed for supersonic flight. Component forces, such as plug force and primary flap boattail drag, will be used to help interpret the effects of the geometric changes on performance. More detailed performance characteristics are presented in appendix B as a function of nozzle pressure ratio and secondary weight flow for all configurations tested.

The assumed turbojet pressure ratio schedule is shown in figure 5. Three subsonic cruise conditions were chosen. They were as follows: Mach 0.80 and a nozzle pressure ratio of 2.35, Mach 0.85 and a pressure ratio of 2.75, and Mach 0.90 and a pressure ratio of 3.1. The supersonic cruise condition was chosen to be Mach 2.7 and a pres-

sure ratio of 27. Since the free-stream Mach number of the Lewis 8- by 6-Foot Supersonic Wind Tunnel is limited to 1.97, the data for the supersonic cruise condition were taken at Mach 1.97 rather than 2.7. However, the configurations of interest have extended outer shrouds in this speed range and are flowing full. Thus, nozzle efficiency is only affected by changes on the external shroud boattail. These changes are relatively small between Mach 1.97 and 2.7.

Effect of Primary Flap Boattail and Nacelle Geometry

Nozzle performance characteristics as influenced by primary flap boattail and nacelle geometry are presented in figure 6 using the assumed turbojet pressure ratio schedule. Data are presented for the full-length plug and a nominal corrected secondary weight flow of 4 percent. For Mach numbers less than 1.0 data are presented for the completely retracted shroud configurations and for Mach numbers greater than 1.2 data are presented for the completely extended shroud configurations.

At subsonic cruise conditions, the nozzle gross thrust coefficient was relatively sensitive to the geometry of the primary flap boattail and nacelle (fig. 6(a)). For example, at Mach 0.90 and a pressure ratio of 3.1, nozzle gross thrust coefficient increased from 0.90 to 0.92 by replacing either the 14° or 17° conical primary flaps and cylindrical nacelle with the larger 14° rounded primary and boattailed nacelle. At Mach 1.97 a thrust coefficient of 1.02 was obtained (plotted at Mach 2.7 in the figure) at a supersonic cruise pressure ratio of 27 with the 17° conical primary. Takeoff gross thrust coefficients for these nozzles ranged from approximately 0.97 to 0.98 at a pressure ratio of 3.0.

Secondary total-pressure recovery requirements are presented in figure 6(b). Since the secondary flow exit was upstream of the primary lip, these nozzles did not pump 4 percent flow from a free-stream source at takeoff.

With the shroud retracted, the 14° rounded primary required higher secondary total pressures than did the conical primaries. When the shroud was extended at supersonic Mach numbers and higher pressure ratios, this trend was reversed.

Primary flap boattail drag was quite low for the nozzle with the 14° rounded primary (fig. 6(c)). For example, at subsonic cruise and a Mach number of 0.90 primary boattail drag was 0.8 percent of ideal thrust. However, with the 17° conical primary, boattail drag increased to 5.3 percent of ideal thrust at the same conditions. With the shroud completely extended at Mach numbers greater than 1.2, primary boattail force became a thrust and was nearly independent of primary boattail shape. For example, at supersonic cruise a thrust of 5 percent of ideal thrust was obtained from the primary boattail surface.

In general, plug thrust was lower when the 14° rounded primary and boattailed nacelle were used instead of the 14° or 17° conical primary and cylindrical nacelle (fig. 6(d)). For example, with subsonic cruise at Mach number of 0.90, plug thrust was 2.7 percent of ideal thrust for the 14° rounded primary. With the 17° conical primary plug thrust amounted to 3.7 percent of ideal thrust. At supersonic cruise the plug thrust of the 17° conical primary nozzle amounted to 4.7 percent of ideal thrust.

Effect of Plug Truncation

The effect of plug truncation on nozzle performance characteristics using the assumed turbojet pressure ratio schedule is presented in figure 7. Data are presented for the 17° conical primary and a nominal corrected secondary weight flow of 4 percent. For Mach numbers less than 1.0 data are shown for the completely retracted shroud configurations (x_c/l_c = -0.116) and for Mach numbers greater than 1.2 data are shown for the completely extended shroud configurations (x_c/l_c = 0.347).

At Mach numbers less than 1.0 with the outer shroud completely retracted, truncation to 50 percent of plug length caused a reduction in performance, particularly at subsonic cruise conditions. For example, at a subsonic cruise pressure ratio of 2.8 and a Mach number of 0.85, gross thrust coefficient decreased from 0.91 to 0.90.

At Mach numbers greater than 1.2 with the outer shroud completely extended, truncation to both 75- and 50-percent plug lengths caused appreciable decrements in gross thrust coefficient, except at supersonic cruise where no appreciable decrement was observed. At supersonic cruise the full-length plug had a gross thrust coefficient of 1.02, while the 50- and 75-percent plugs both had slightly lower gross thrust coefficients.

Truncation of the plug had no effect on pumping characteristics of these nozzles as can be seen from figure 7(b). Truncation of the plug also had no effect on primary flap boattail drag (fig. 7(c)). However, truncation did decrease plug forces in general (fig. 7(d)). Plug base forces were generally positive (i.e., a thrust) and were less than 1 percent of the primary jet thrust.

Figure 8 presents a comparison of performance characteristics for the open and closed plug base for the 50-percent truncated plug. For this comparison the 17° conical primary was used and the shroud was completely extended (x_c/l_c = 0.347). Corrected secondary flow was maintained at a nominal 4 percent. For the open-base configuration a small portion of the secondary flow was allowed to flow through the hollow support struts to the plug base to provide base bleed. Nozzle gross thrust coefficients were comparable for the open and closed base configurations (fig. 8(a)). Pumping characteristics for these nozzles were also comparable (fig. 8(b)). In addition, all of the component forces were comparable and apparently insensitive to whether the base was open or closed (figs. 8(c) to (e)).

Effect of Shroud Geometry

The effect of shroud length on nozzle performance characteristics for the 17° conical primary, full-length plug is shown in figure 9. Corrected secondary weight flow was again maintained at a nominal 4 percent. At Mach numbers less than 1.0, nozzle gross thrust coefficient was comparable for the two retracted-shroud configurations (x_c/l_c = -0.116 and x_c/l_c = -0.076) except at takeoff and subsonic cruise (fig. 9(a)). At takeoff with the shroud at x_c/l_c = -0.116 the gross thrust coefficient was approximately 0.97. For the subsonic cruise conditions, gross thrust coefficient was higher with the shroud at x_c/l_c = -0.116 than with it at x_c/l_c = -0.076. At supersonic cruise with the shroud extended to x_c/l_c = 0.347, gross thrust coefficient was 1.02. For the range of shroud extensions which were tested, there was little effect on pumping characteristics (fig. 9(b)).

At subsonic cruise conditions primary boattail drag was lower and plug thrust higher with the external shroud at x_c/l_c = -0.116 than with it at x_c/l_c = -0.076 (figs. 9(c) and (d)). This accounts for the higher gross thrust coefficients when the shroud was completely retracted. At supersonic cruise, boattail force was a thrust and was comparable for the intermediate shroud (x_c/l_c = 0.223) and the completely extended shroud (x_c/l_c = 0.347). However, the plug thrust was higher for the completely extended shroud and higher overall performance was achieved.

The effect of shroud length on nozzle performance characteristics for the 14° rounded primary, full-length plug is shown in figure 10. Corrected secondary weight flow was again maintained at a nominal 4 percent. In general, at Mach numbers less than 1.0 nozzle efficiency was highest for the configuration with the completely retracted shroud (x_r/l_r = -0.167) (fig. 10(a)). This was particularly true at subsonic cruise conditions where extensions of the outer shroud caused large decrements in gross thrust coefficient. For example, at Mach 0.90 and a nozzle pressure ratio of 3.1, gross thrust coefficient was 0.92 with the shroud completely retracted. With the shroud extended to x_r/l_r = 0.011, gross thrust coefficient dropped to 0.90. A further extension of the shroud to x_r/l_r = 0.182 decreased gross thrust coefficient to 0.86. At Mach numbers greater than 1.2, gross thrust coefficient of the completely extended shroud (x_r/l_r = 0.366) was consistently higher than that of the intermediate shroud at x_r/l_r = 0.182.

Pumping characteristics at takeoff were sensitive to the location of the shroud. As expected, there was no pumping with a fully retracted shroud. Extending the shroud to x_r/l_r = 0.182, however, provided some cooling flow with little effect on performance. At Mach numbers less than 1.2 as the shroud was extended, the pressure levels in the secondary passage decreased. Thus gross thrust coefficients were adversely affected due to reduced secondary air momentum. As the shroud was extended at Mach numbers less than 1.0, boattail drag increased (fig. 10(c)) and plug thrust decreased (fig. 10(d)).

These changes in the component forces, combined with the loss in secondary momentum, were responsible for the large decrements in gross thrust coefficient observed as the shroud was extended.

At Mach numbers greater than 1.2, the configuration with the completely extended shroud ($x_r/l_r = 0.366$) consistently had lower primary boattail drags and higher plug forces than with the intermediate shroud ($x_r/l_r = 0.182$). The effect of the flared nacelle on nozzle performance characteristics of the 17° conical primary, full-length plug is shown in figure 11. Corrected secondary weight flow was a nominal 4 percent. Results are compared with the cylindrical nacelle. The shrouds were located at $x_c/l_c = -0.076$ for the cylindrical nacelle and $x_c/l_c = -0.087$ for the flared nacelle. The nozzle gross thrust coefficient presented for this configuration does not include the force on the forward-facing surface. This force was determined from a pressure integration and added to the nozzle thrust-minus-drag determined from the load cell. In general, the gross thrust coefficient of the nozzle with the cylindrical nacelle (fig. 11(a)) was higher than that of the nozzle with the flared nacelle except at subsonic cruise where the opposite trend occurred. In general, the pressure levels in the secondary flow passage (fig. 11(b)) were higher for the flared nacelle, particularly at subsonic cruise.

The presence of the flared nacelle tended to decrease boattail drag (fig. 11(c)) and increase plug thrust (fig. 11(d)) when compared with the component forces of the cylindrical nacelle. For example, at a subsonic cruise Mach number of 0.90, boattail drag was decreased from approximately 6 to 2 percent of ideal thrust when the flared nacelle was used. In addition, plug thrust was increased from 3 to 4.8 percent. However, these favorable effects of flaring the nacelle were largely offset by the drag incurred on the rearward-facing surface of the flare (fig. 11(e)). Thus the net effect of the flared nacelle was to increase gross thrust coefficient at subsonic cruise and to decrease it over the acceleration schedule. The force on the forward-facing surface of the flare was generally small and was a thrust at subsonic Mach numbers from 0.60 to 0.95 (fig. 11(f)).

SUMMARY OF RESULTS

An experimental investigation was conducted to determine the performance characteristics of several 10° half-angle conical plug nozzles. Comparisons were made between three nozzles with various primary flap and nacelle configurations to determine the effect of these geometric variables on performance. In addition, the effect of plug truncation on performance was also evaluated. Secondary flow was varied from approximately 0 to 10 percent of primary weight flow. Internal expansion was varied by translation of a cylindrical secondary shroud. The following results were obtained:

For supersonic cruise:

1. A nozzle gross thrust coefficient of 1.02 was obtained at Mach 1.97 at a supersonic cruise pressure ratio of 27 with a 17° conical primary and a full-length plug. The shroud was extended and the corrected secondary weight-flow ratio had a nominal value of 4 percent. For this configuration the primary flap and plug thrusts were, respectively, 5 and 4.8 percent of the ideal thrust.

2. Truncation of the plug had no appreciable effect on gross thrust coefficient.

For subsonic cruise:

1. With the shroud retracted, the nozzle gross thrust coefficient was sensitive to the geometry of the nacelle and the primary nozzle flap. For example, at Mach 0.9 for a pressure ratio of 3.1 and a corrected secondary weight-flow ratio of 4 percent nozzle gross thrust coefficient increased from 0.90 to 0.92 by replacing either a smaller 14° or 17° conical primary and cylindrical nacelle with a larger 14° rounded primary and boattailed nacelle. Primary boattail drag was 5.3 percent of ideal thrust for the 17° conical primary and 0.8 percent of ideal thrust for the 14° rounded primary.

2. Truncation to 50 percent of plug length caused a reduction in performance. For example, at a pressure ratio of 2.8 and a Mach number of 0.85, nozzle gross thrust coefficient dropped from 0.91 to 0.90. This loss resulted from a reduction in the plug thrust.

For takeoff:

1. Takeoff nozzle gross thrust coefficients ranged from approximately 0.97 to 0.98 at a pressure ratio of 3.0 and a corrected secondary weight-flow ratio of 0.04.

2. Pumping characteristics were sensitive to the location of the shroud. As expected, there was no pumping with a fully retracted shroud. Extending the shroud to 18 percent of the plug length, however, provided some cooling flow with little effect on performance.

Lewis Research Center,
National Aeronautics and Space Administration,
Cleveland, Ohio, June 22, 1970,
720-03.

APPENDIX A

SYMBOLS

A	area
C_{fg}	nozzle gross thrust coefficient, $(F - D)/F_{ip}$
D	drag
$D_{F, F}$	flared nacelle drag (forward-facing surface)
$D_{F, R}$	flared nacelle drag (rearward-facing surface)
F	nozzle gross thrust
F_{pl}	nozzle plug thrust
l	plug length measured from nozzle throat to plug tip
M	Mach number
P	total pressure
p	static pressure
T	total temperature
u_1	external shroud position coordinate (axial)
u_2	external shroud position coordinate (radial)
w	weight flow rate
$\frac{w_s}{w_p}\sqrt{\frac{T_s}{T_p}}$	corrected secondary weight flow ratio
x	axial distance measured downstream of nozzle throat
y	distance measured along primary rake from primary airflow passage wall
z_1	14^o rounded primary position coordinate (axial)
z_2	14^o rounded primary position coordinate (radial)
α	primary nozzle boattail angle
φ	circumferential angle measured from top of nacelle in a clockwise direction (looking upstream)

Subscripts:

b	plug base
c	conical primaries
i	ideal
m	nacelle
p	primary air
pl	plug
r	14^o rounded primary
s	secondary air
β	boattail surface
0	free-stream
7	nozzle inlet station
8	nozzle throat station
9	nozzle exit station

APPENDIX B

NOZZLE PERFORMANCE CHARACTERISTICS

Nozzle Pressure Ratio Effects

The effect of nozzle pressure ratio on nozzle performance characteristics is shown in figures 12 to 26 for all configurations tested. Corrected secondary weight flow was maintained at a nominal 4 percent while pressure ratio was varied at a given Mach number. Nozzle gross thrust coefficient was nearly independent of Mach number for the extended shroud nozzles (x_c/l_c or x_r/l_r is positive) at Mach numbers greater than 1.2. For all configurations with retracted shrouds (x_c/l_c or x_r/l_r is negative) at pressure ratios below 9, secondary total pressure was about equal to or less than the ambient static pressure. For the extended shroud configurations above a pressure ratio of 8, the secondary total pressure ratio was insensitive to variations in nozzle pressure ratio. This was due to the secondary flow being aerodynamically choked by the primary flow, which attached to the extended shroud at high pressure ratios. This phenomenon is explained more fully in reference 10.

Secondary Flow Effects

The effect of corrected secondary weight flow ratio on nozzle performance characteristics is presented in figures 27 to 41 for all configurations tested. Nozzle gross thrust coefficient increased with increasing secondary flow and peaked at 10-percent corrected secondary weight flow for all configurations tested.

For the retracted-shroud nozzles, geometric choking of the secondary air occurred only at the higher secondary weight flows and for pressure ratios greater than 5. Generally for extended shroud configurations, the secondary total pressure ratio (P_s/P_7) was independent of nozzle pressure ratio at all secondary weight flows, indicating that the secondary air was aerodynamically choked. Geometric choking of the secondary flow occurred at corrected secondary weight flows above 6 percent for the extended shroud nozzles.

REFERENCES

1. Valerino, Alfred S.; Zappa, Robert F.; and Abdalla, Kaleel L.: Effects of External Stream on the Performance of Isentropic Plug-Type Nozzles at Mach Numbers of 2.0, 1.8, and 1.5. NASA Memo 2-17-59E, 1959.

2. Salmi, Reino J.: Preliminary Investigation of Methods to Increase Base Pressure of Plug Nozzles at Mach 0.9. NACA RM E56J05, 1965.

3. Salmi, Reino J.; and Cortright, E. M., Jr.: Effects of External Stream Flow and Afterbody Variations on the Performance of a Plug Nozzle at High Subsonic Speeds. NACA RM E56F11a, 1956.

4. Schmeer, James W.; Kirkham, Frank S.; and Salters, Leland B., Jr.: Performance Characteristics of a 10^{o} Conical Plug Nozzle at Mach Numbers up to 1.29. NASA TM X-913, 1964.

5. Herbert, M. V.; Golesworthy, G. T.; and Herd, R. J.: The Performance of a Centre Body Propelling Nozzle With a Parallel Shroud in External Flow, Part II. Rep. ARC-CP-894, Aeronautical Research Council, Great Britain, 1966.

6. Bresnahan, Donald L.; and Johns, Albert L.: Cold Flow Investigation of a Low Angle Turbojet Plug Nozzle With Fixed Throat and Translating Shroud at Mach Numbers From 0 to 2.0. NASA TM X-1619, 1968.

7. Wasko, Robert A.; and Harrington, Douglas E.: Performance of a Collapsible Plug Nozzle Having Either Two-Position Cylindrical or Variable Angle Floating Shrouds at Mach Numbers From 0 to 2.0. NASA TM X-1657, 1968.

8. Bresnahan, Donald L.: Experimental Investigation of a 10^{o} Conical Turbojet Plug Nozzle With Iris Primary and Translating Shroud at Mach Numbers From 0 to 2.0. NASA TM X-1709, 1968.

9. Johns, Albert L.: Quiescent-Air Performance of a Truncated Turbojet Plug Nozzle With Shroud and Plug Base Flows From a Common Source. NASA TM X-1807, 1969.

10. Bresnahan, Donald L.: Experimental Investigation of a 10^{o} Conical Plug Nozzle With Translating Primary and Secondary Shrouds at Mach Numbers From 0 to 2.0. NASA TM X-1777, 1969.

11. Huntley, Sidney C.; and Samanich, Nick E.: Performance of a 10^{o} Conical Plug Nozzle Using a Turbojet Gas Generator. NASA TM X-52570, 1969.

12. Wilcox, Fred A.; Samanich, Nick E.; and Blaha, Bernard J.: Flight and Wind Tunnel Investigation of Installation Effects on Supersonic Cruise Exhaust Nozzles at Transonic Speeds. Paper 69-427, AIAA, June 1969. (Also available as NASA TM X-52586, 1969.)

13. Smith, K. G.: Methods and Charts for Estimating Skin Friction Drag in Wind Tunnel Tests With Zero Heat Transfer. Rep. ARC-CP-824, Aeronautical Research Council, Great Britain, 1965.

14. Harrington, Douglas E.: Jet Effects on Boattail Pressure Drag of Isolated Ejector Nozzles at Mach Numbers From 0.60 to 1.47. NASA TM X-1785, 1969.

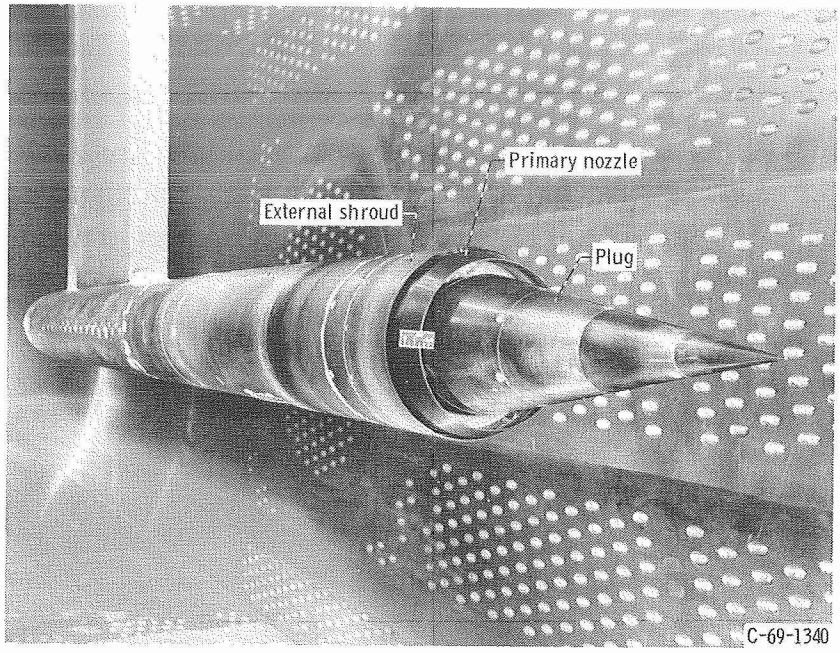

Figure 1. - Model installed in 8- by 6-Foot Supersonic Wind Tunnel.

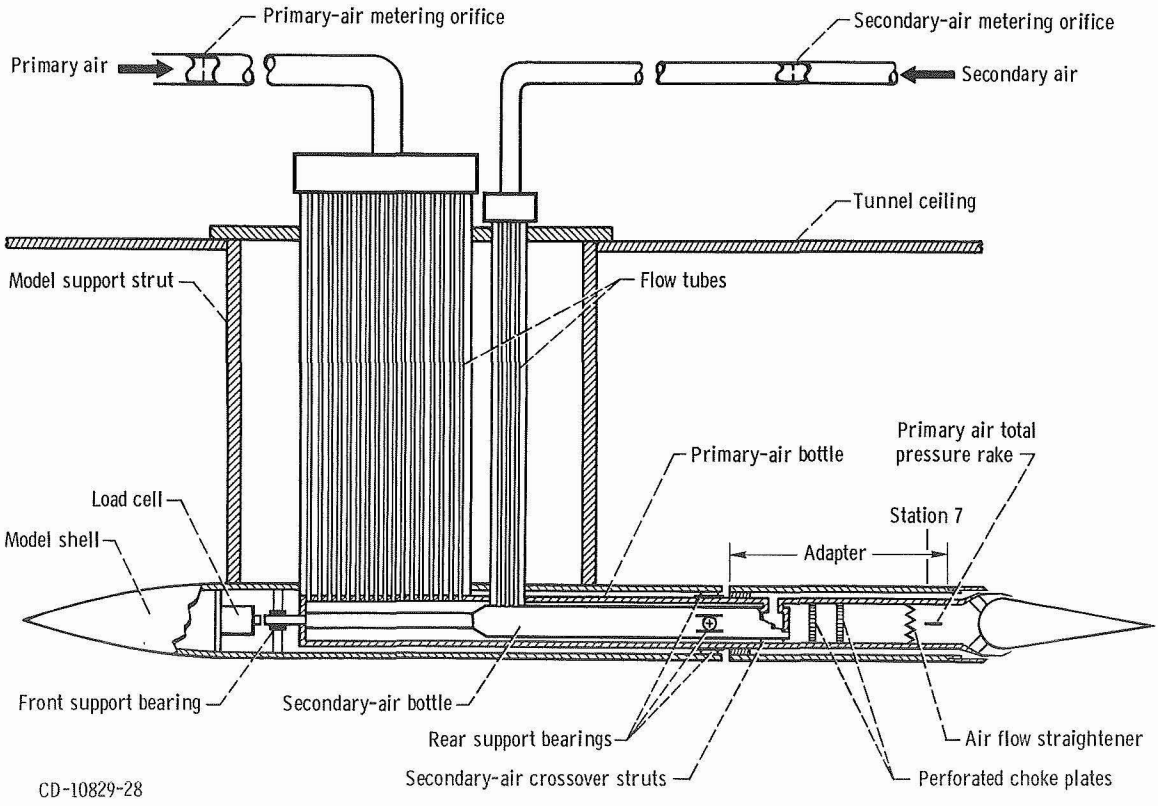

Figure 2. - Model internal geometry and thrust-measuring system.

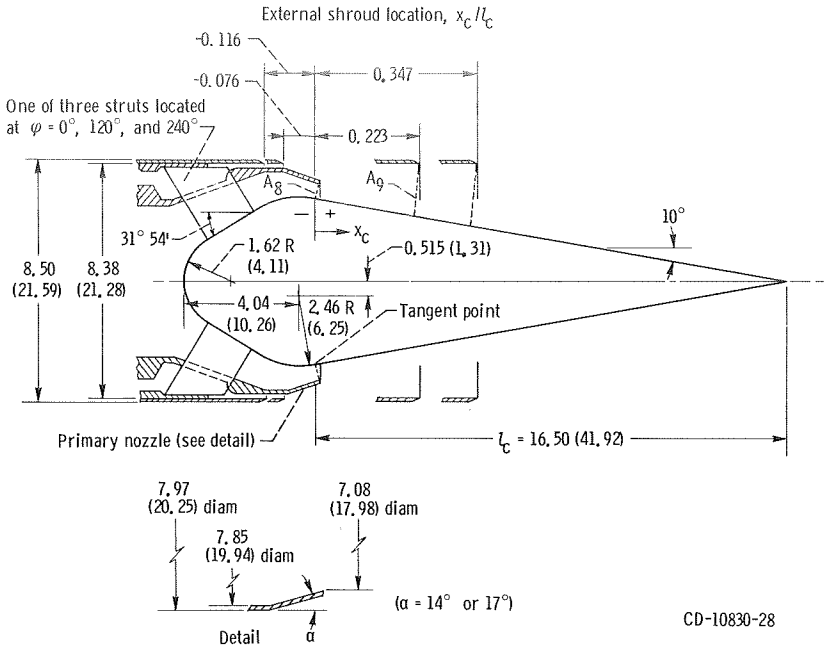

(a) Plug nozzle cylindrical shroud locations for conical primaries (see table I for shroud variables).

Rounded primary position coordinates		
z_1, in. (cm)	z_2, in. (cm)	
0 (0)	0 (0)	Straight line
2.31 (5.87)	.58 (1.47)	
2.65 (6.74)	.65 (1.65)	
2.99 (7.60)	.71 (1.80)	
3.33 (8.46)	.77 (1.96)	
4.01 (10.19)	.86 (2.18)	
4.35 (11.05)	.90 (2.29)	
4.83 (12.27)	.93 (2.36)	
5.03 (12.78)	.94 (2.39)	

External shroud position coordinates	
u_1, in. (cm)	u_2, in. (cm)
0 (0)	0 (0)
.34 (.86)	.07 (.19)
.68 (1.73)	.15 (.37)
1.02 (2.59)	.21 (.52)
1.36 (3.45)	.26 (.65)
1.70 (4.32)	.30 (.76)
2.04 (5.18)	.33 (.84)
2.35 (5.97)	.34 (.87)

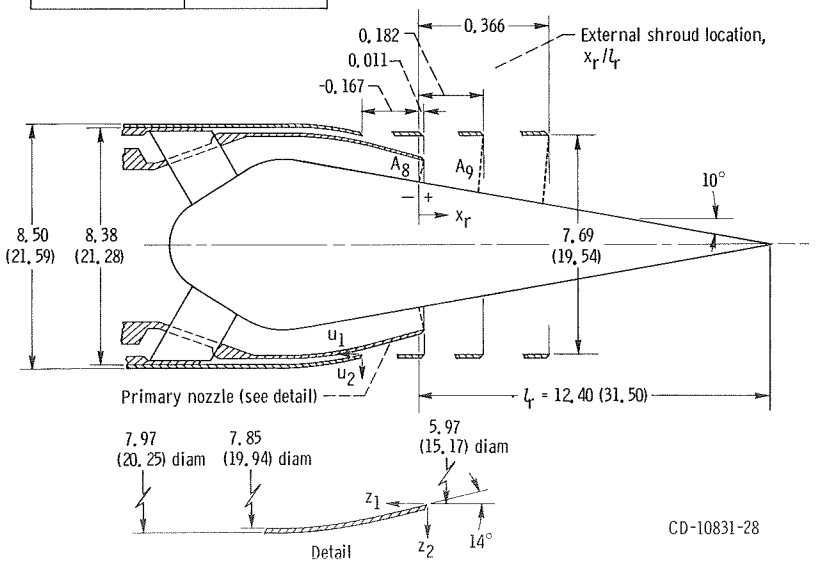

(b) Plug nozzle shroud locations for 14° rounded primary (see table I for shroud variables).

Figure 3. - Model dimensions and geometric variables. All dimensions are in inches (cm).

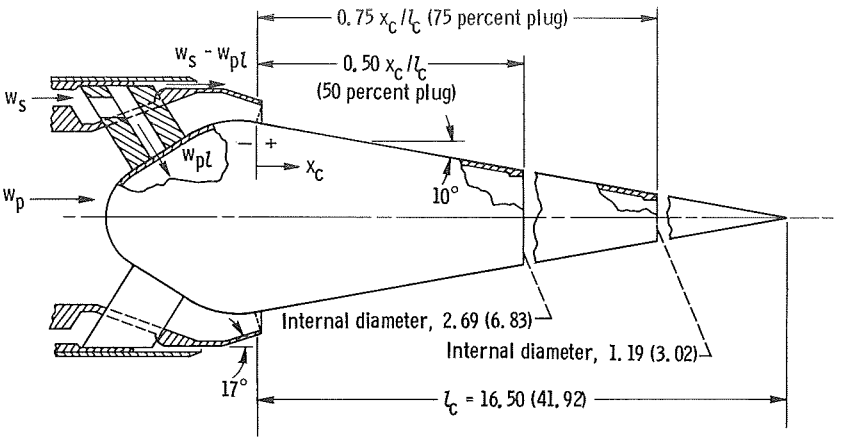

(c) Plug nozzle truncations.

CD-10832-28

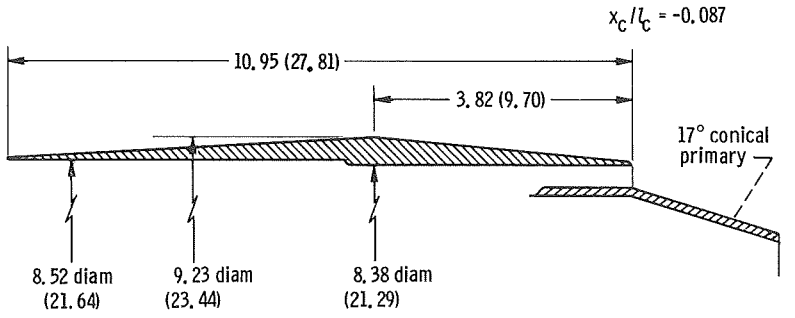

(d) Flared nacelle.

CD-10833-28

Figure 3. - Concluded.

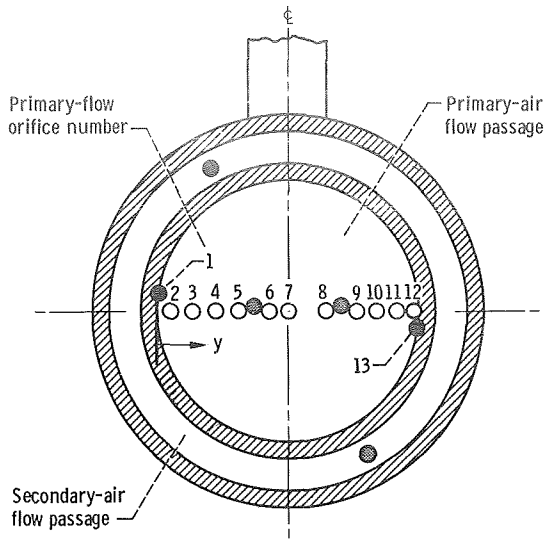

Primary flow orifice number	Distance, y, in. (cm)
1	0 (0)
2	.29 (0.74)
3	.61 (1.55)
4	.98 (2.49)
5	1.43 (3.63)
6	2.10 (5.34)
7	3.00 (7.61)
8	4.28 (10.88)
9	4.81 (12.21)
10	5.23 (13.28)
11	5.56 (14.12)
12	5.87 (14.90)
13	6.01 (15.27)

○ Total-pressure orifice
● Static-pressure orifice
◍ Thermocouple

(a) Station 7 instrumentation.

CD-10834-28

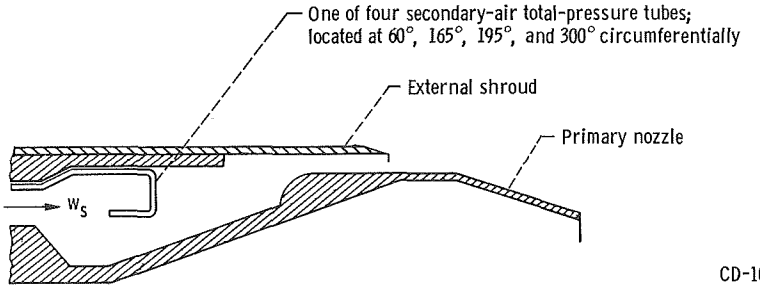

CD-10835-28

(b) Secondary-air total-pressure instrumentation.

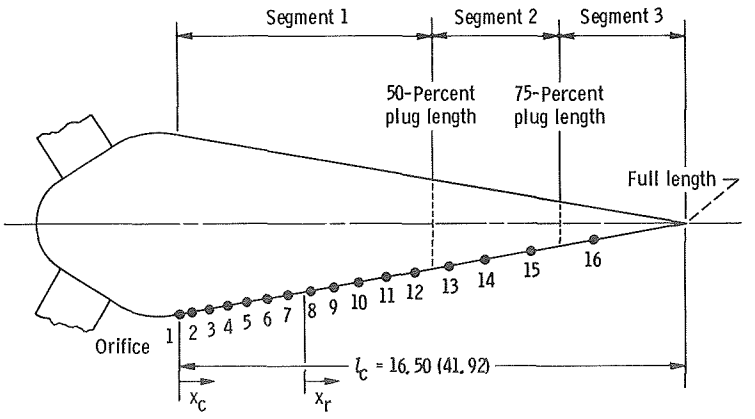

Orifice	x_c, in. (cm)	x_c / l_c
1	0 (0)	0
2	.33 (.84)	.02
3	.91 (2.31)	.06
4	1.51 (3.84)	.09
5	2.14 (5.44)	.13
6	2.79 (7.09)	.17
7	3.48 (8.84)	.21
8	4.21 (10.69)	.25
9	4.98 (12.65)	.30
10	5.81 (14.76)	.35
11	6.70 (17.02)	.41
12	7.69 (19.53)	.47
13	8.75 (22.23)	.53
14	9.96 (25.30)	.60
15	11.44 (29.06)	.69
16	13.56 (34.44)	.82

(c) Plug-surface static-pressure locations (circumferential location, φ = 180°).

CD-10836-28

Figure 4. - Model instrumentation. All dimensions are in inches (cm).

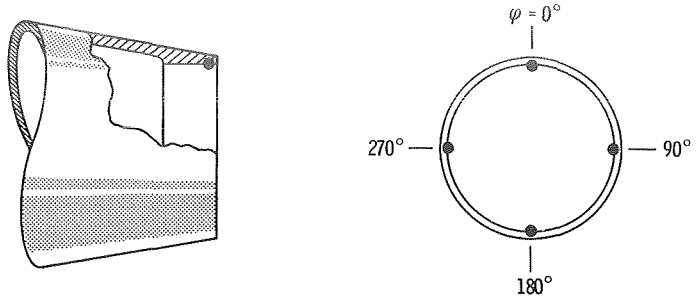

(d) Base static pressures for truncated plugs (open base).

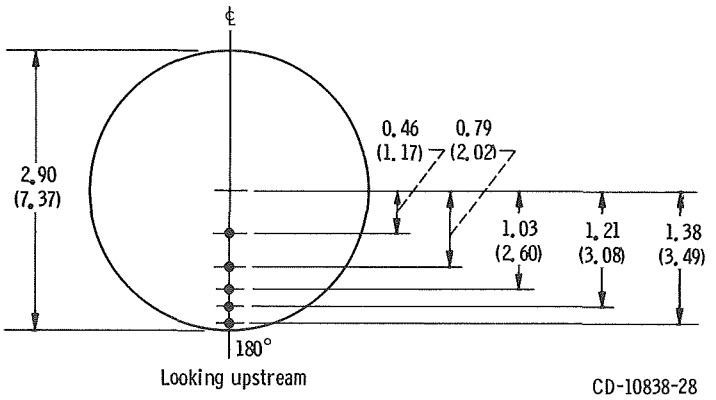

(e) Plug-base static pressures (50-percent plug, closed base).

Figure 4. - Continued.

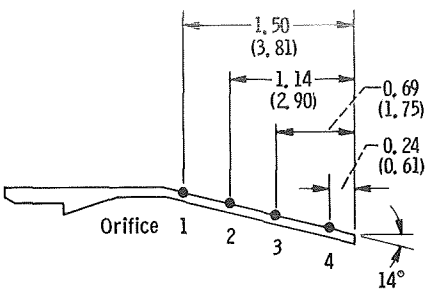

14° conical primary

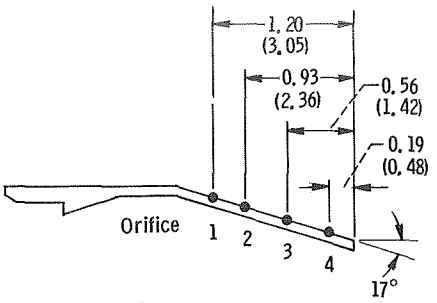

17° conical primary

Orifice	Circumferential location, φ, deg
1	30
2	45
3	75
4	90

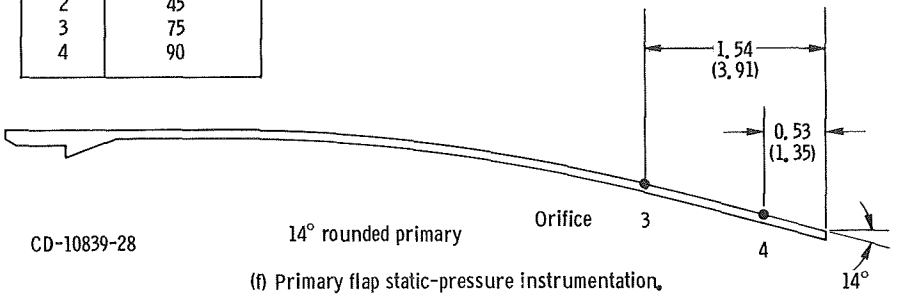

CD-10839-28

14° rounded primary

(f) Primary flap static-pressure instrumentation.

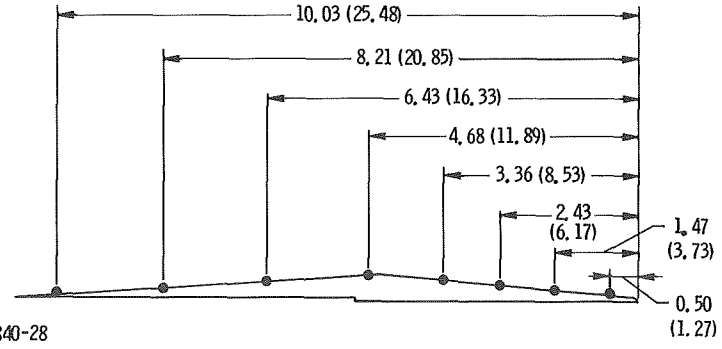

CD-10840-28

(g) Flared nacelle static-pressure instrumentation (circumferential location, $\varphi = 180°$).

Figure 4. - Concluded.

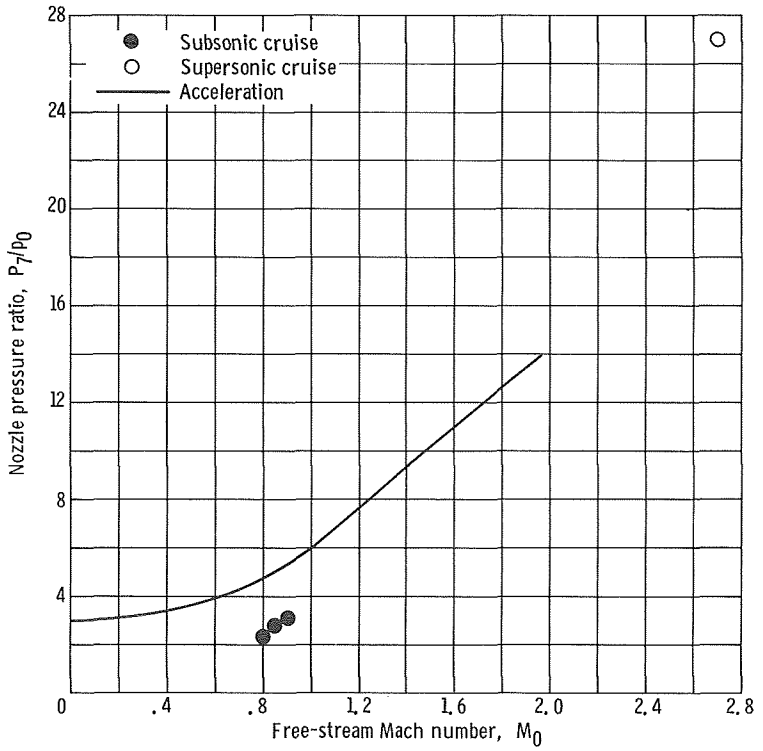

Figure 5. - Assumed turbojet pressure ratio schedule.

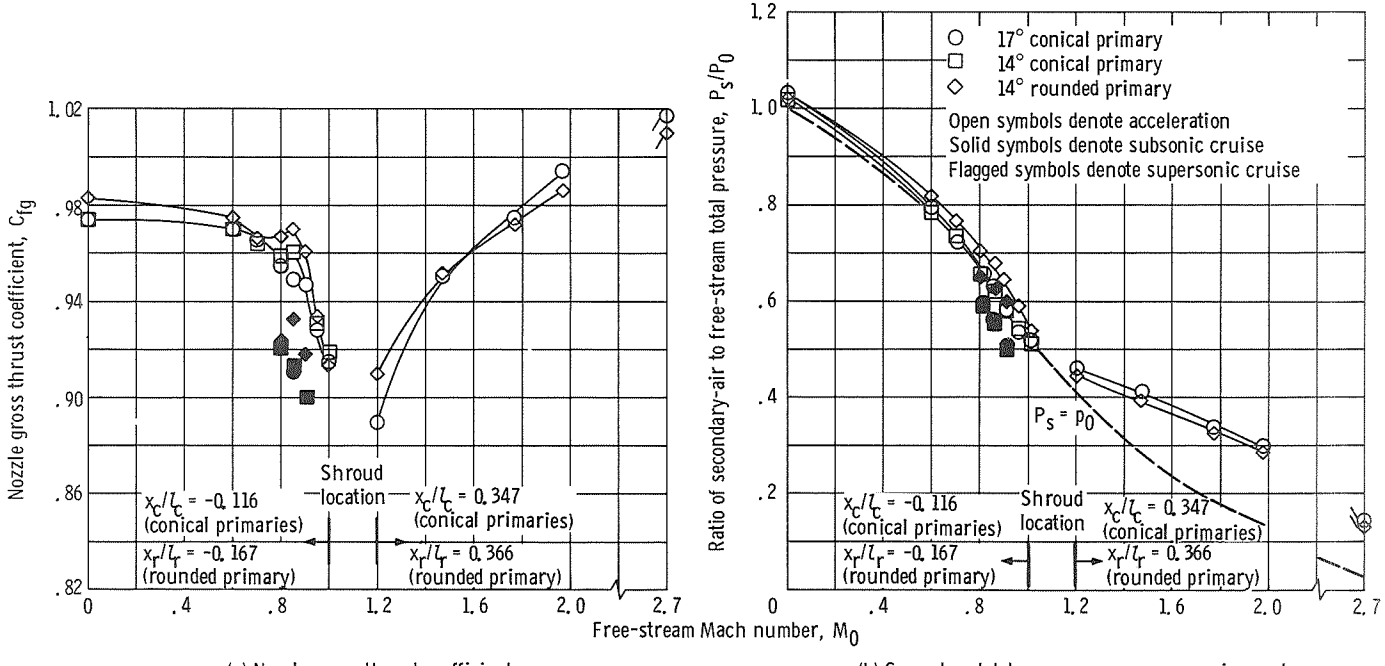

(a) Nozzle gross thrust coefficient.

(b) Secondary total-pressure recovery requirements.

Figure 6. - Comparison of nozzle characteristics. Full-length plug; corrected secondary weight flow ratio, $(w_s/w_p)\sqrt{T_s/T_p} = 0.04$.

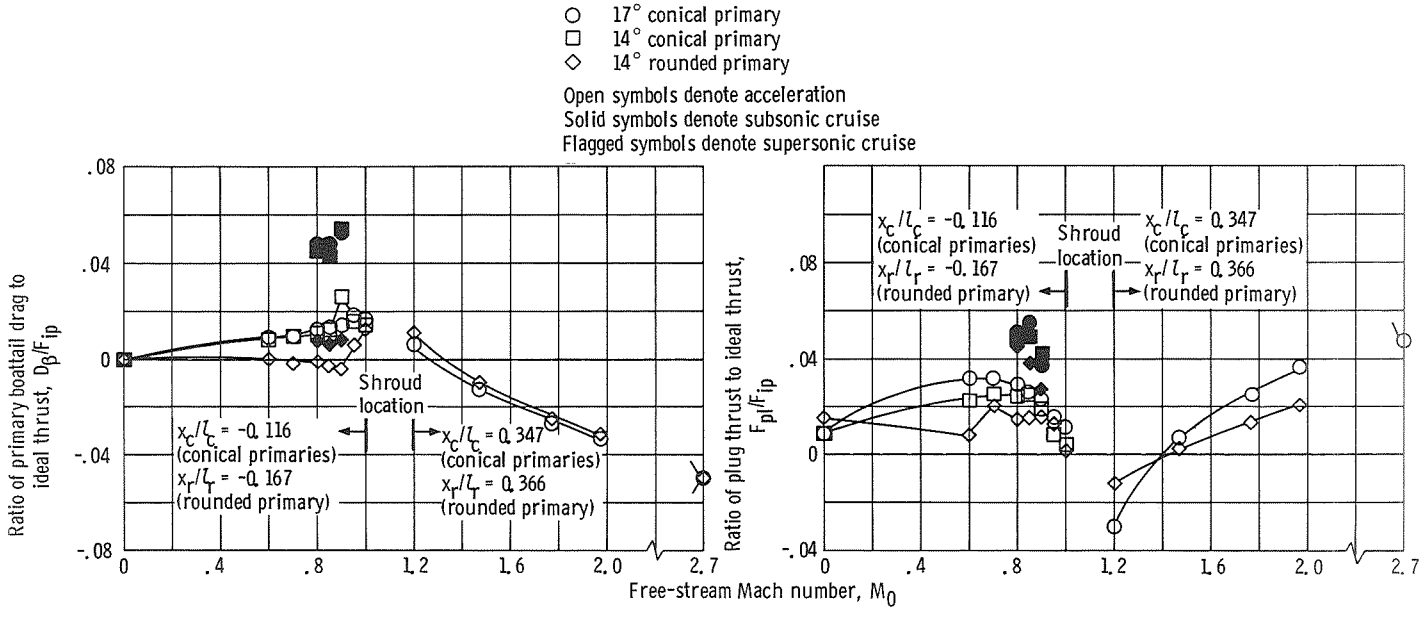

(c) Primary flap drag.

(d) Plug thrust.

Figure 6. - Concluded.

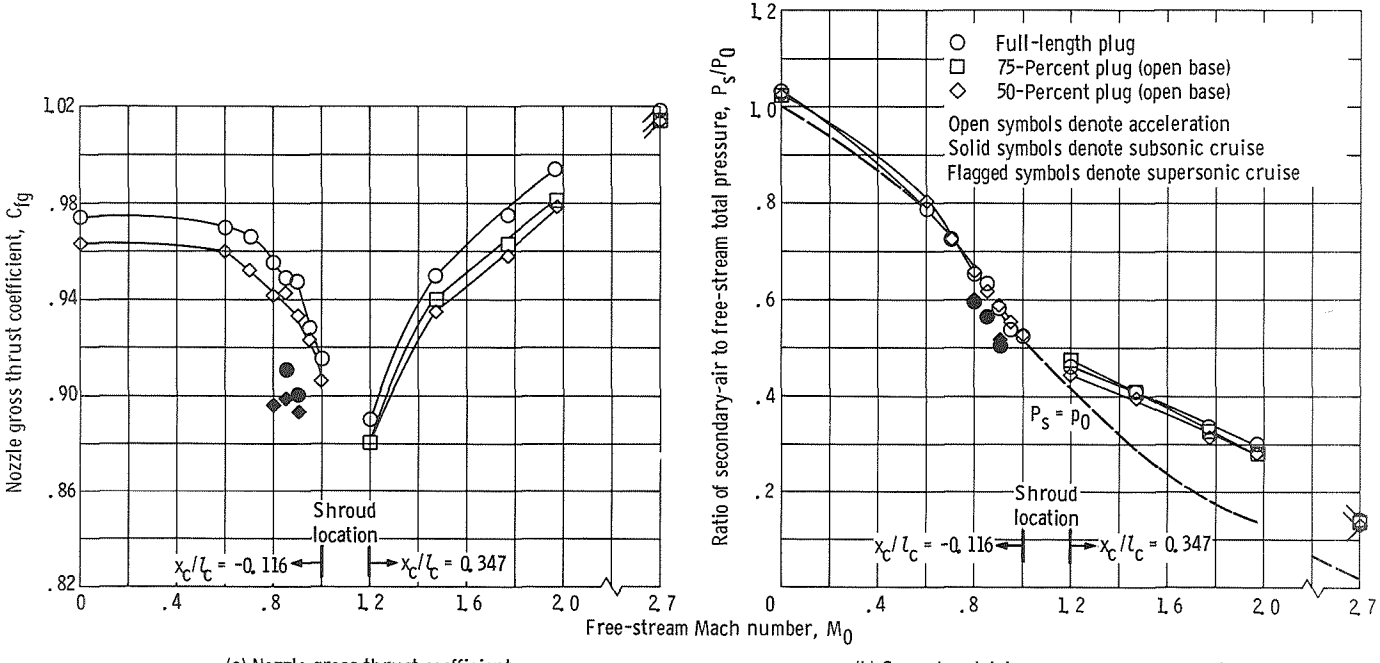

(a) Nozzle gross thrust coefficient.

(b) Secondary total-pressure recovery requirements.

Figure 7. - Effect of plug truncation on nozzle performance characteristics. 17° conical primary; corrected secondary weight flow ratio, $(w_s/w_p)\sqrt{T_s/T_p}$ = 0.04.

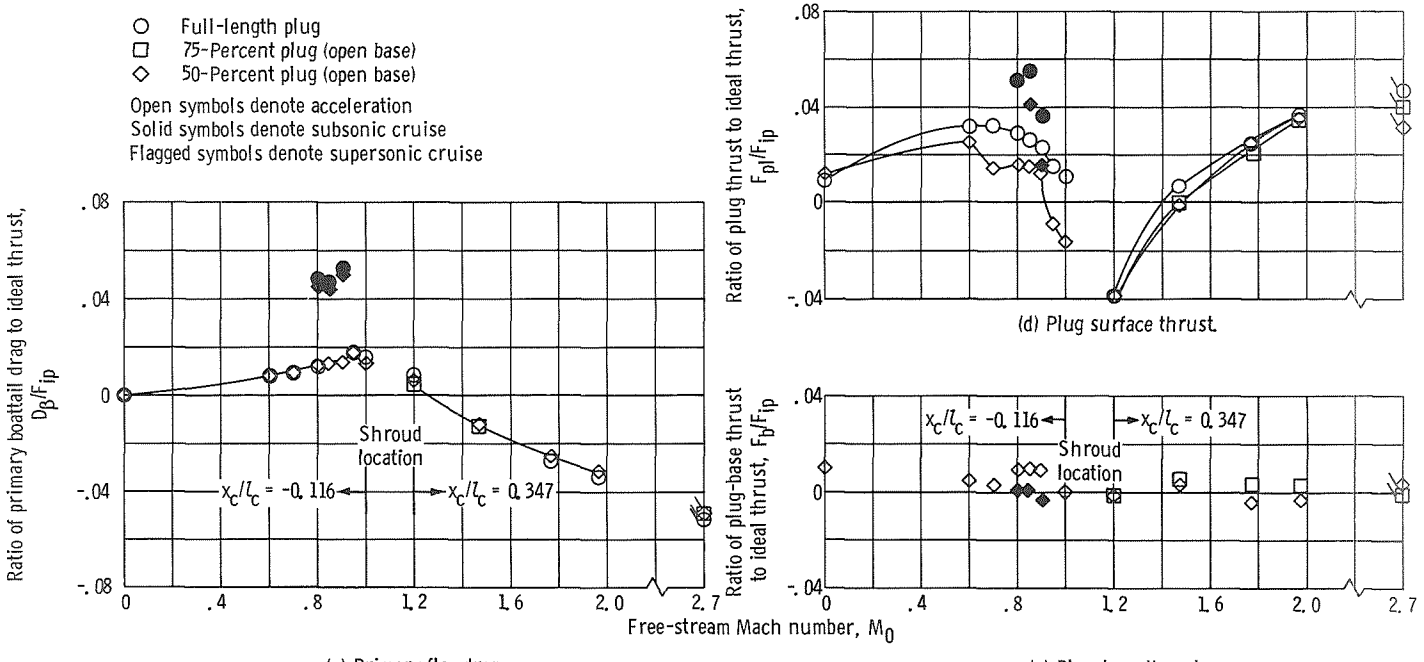

(c) Primary flap drag.

(d) Plug surface thrust.

(e) Plug-base thrust.

Figure 7. - Concluded.

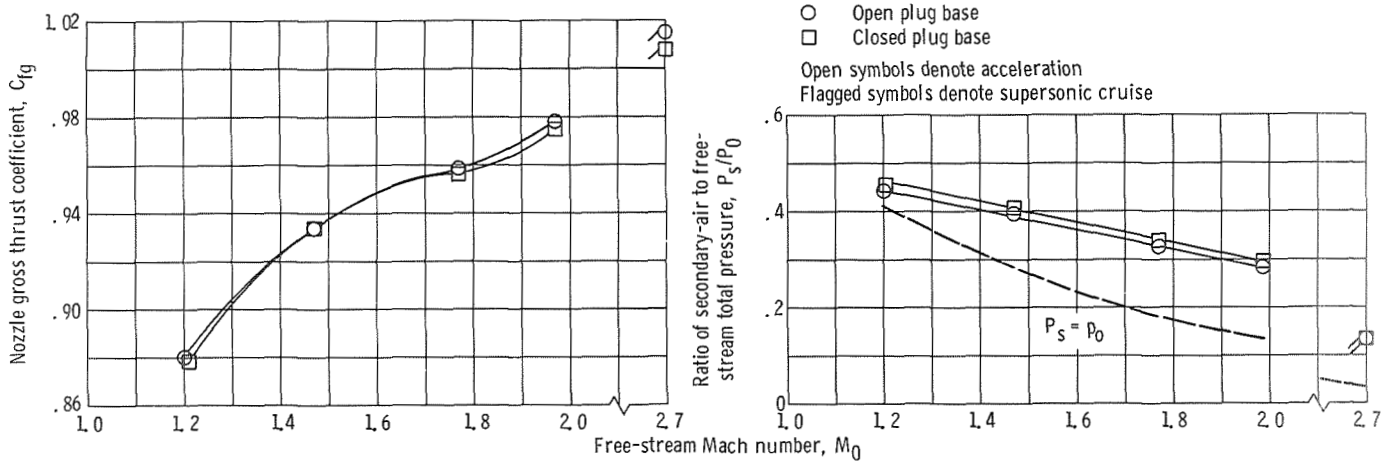

(a) Nozzle gross thrust coefficient.

(b) Secondary total-pressure recovery requirements.

Figure 8. - Comparison between open and closed plug base performance characteristics. 50-Percent plug; shroud location, $x_c/l_c = 0.347$; 17° conical primary; corrected secondary weight flow ratio, $(w_s/w_p)\sqrt{T_s/T_p} = 0.04$.

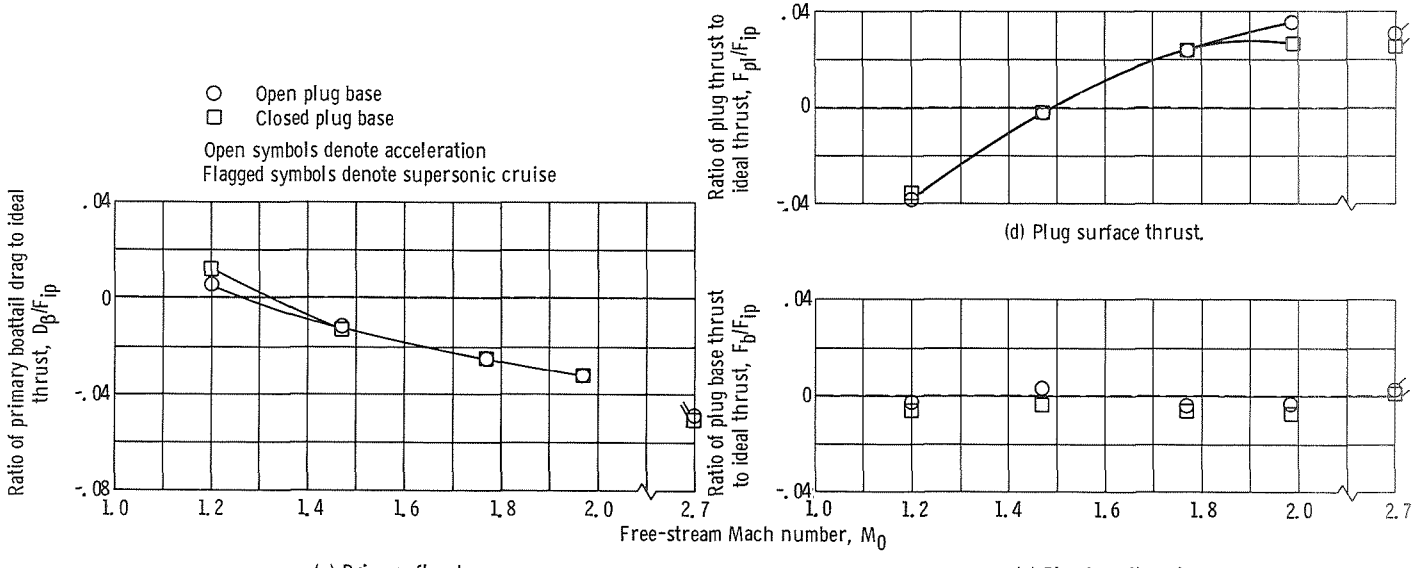

(c) Primary flap drag.

(d) Plug surface thrust.

(e) Plug base thrust.

Figure 8. - Concluded.

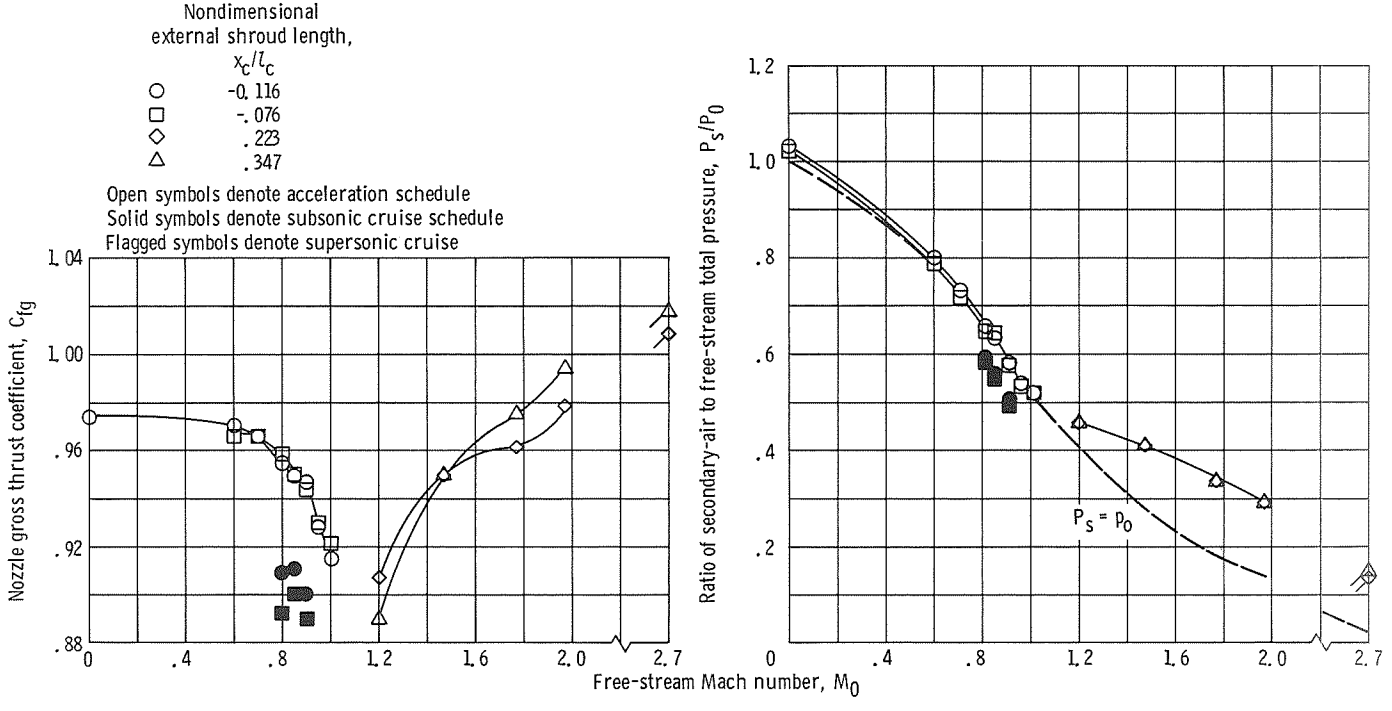

(a) Nozzle gross thrust coefficient.

(b) Secondary total-pressure requirements.

Figure 9. - Effect of external shroud length on nozzle performance characteristics. Full-length plug; 17° conical primary; corrected secondary weight flow ratio, $(w_s/w_p)\sqrt{T_s/T_p} = 0.04$.

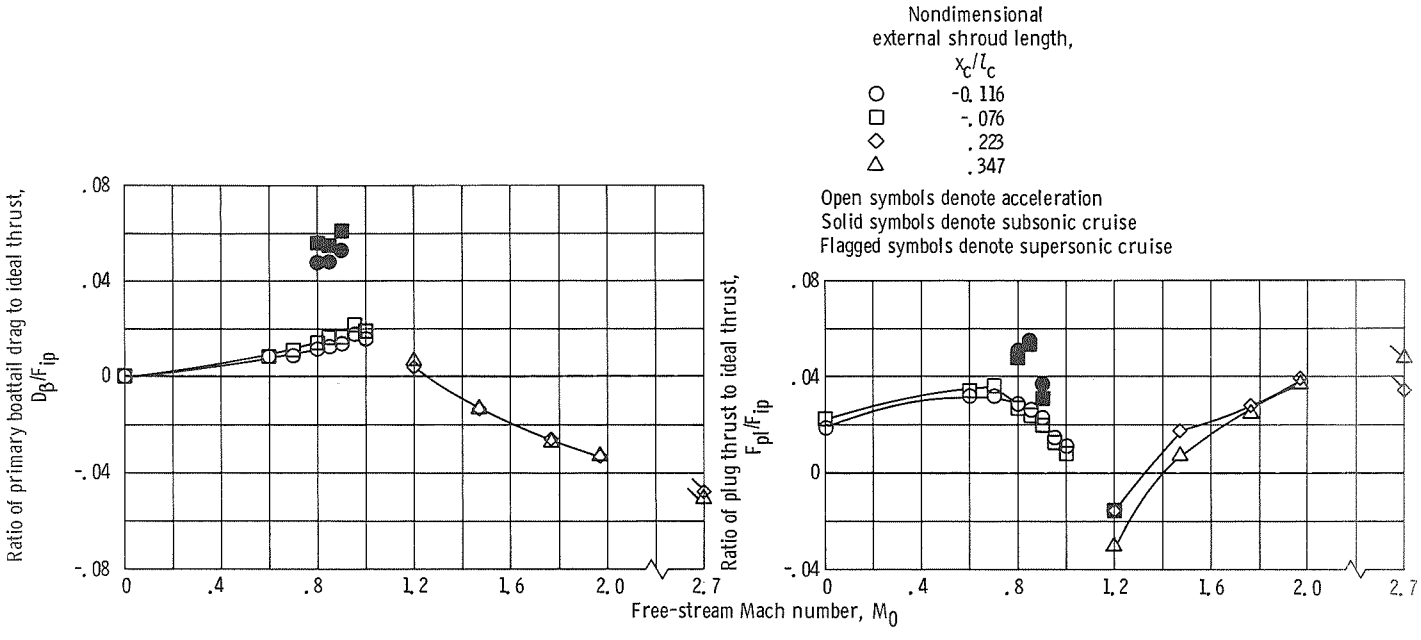

(c) Primary flap drag.

(d) Plug surface thrust.

Figure 9. - Concluded.

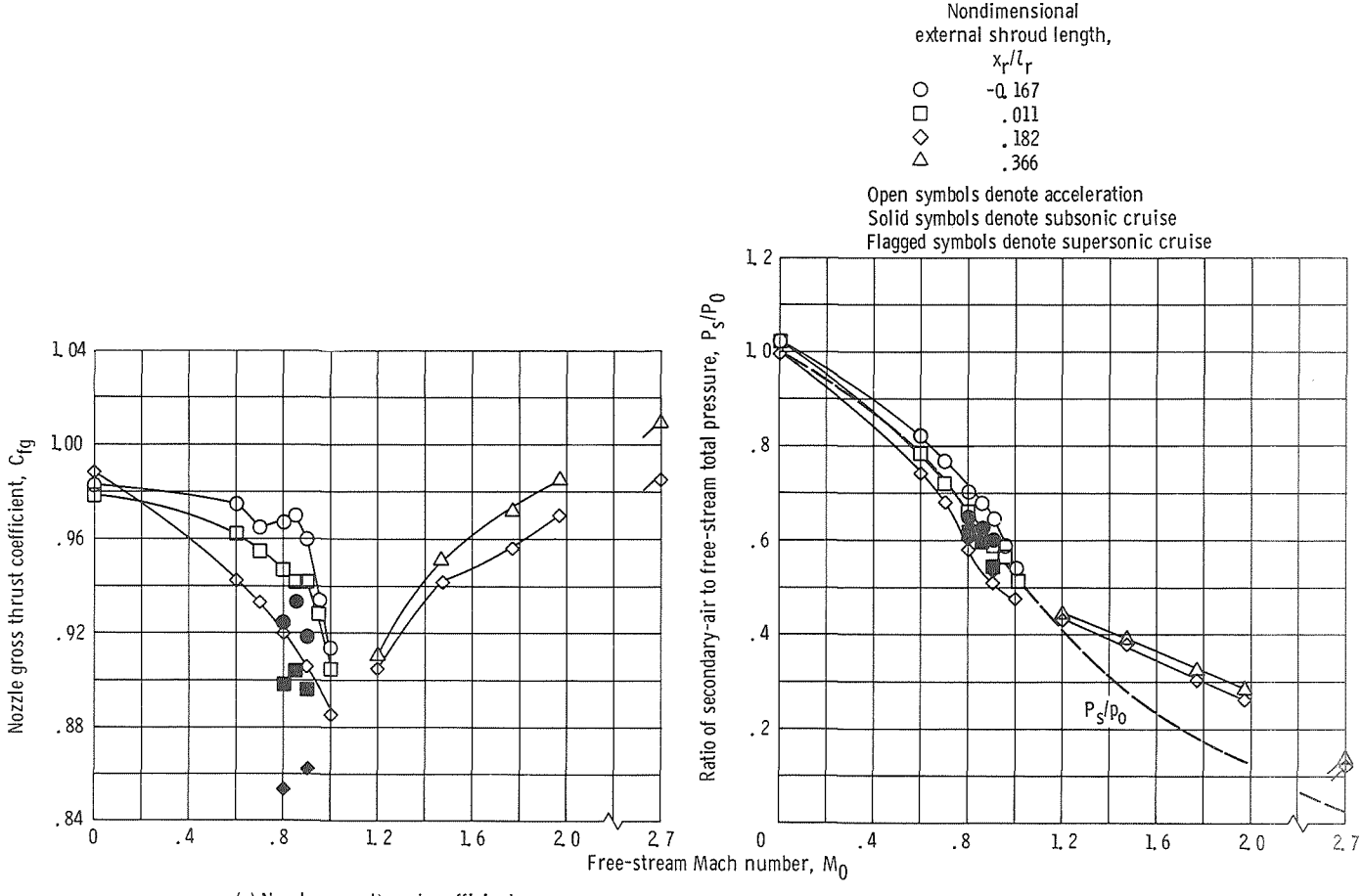

(a) Nozzle gross thrust coefficient.

(b) Secondary total-pressure recovery requirements.

Figure 10. - Effect of external shroud length on nozzle performance characteristics. Full length plug; 14° rounded primary; corrected secondary weight flow ratio, $(w_s/w_p)\sqrt{T_s/T_p} = 0.64$.

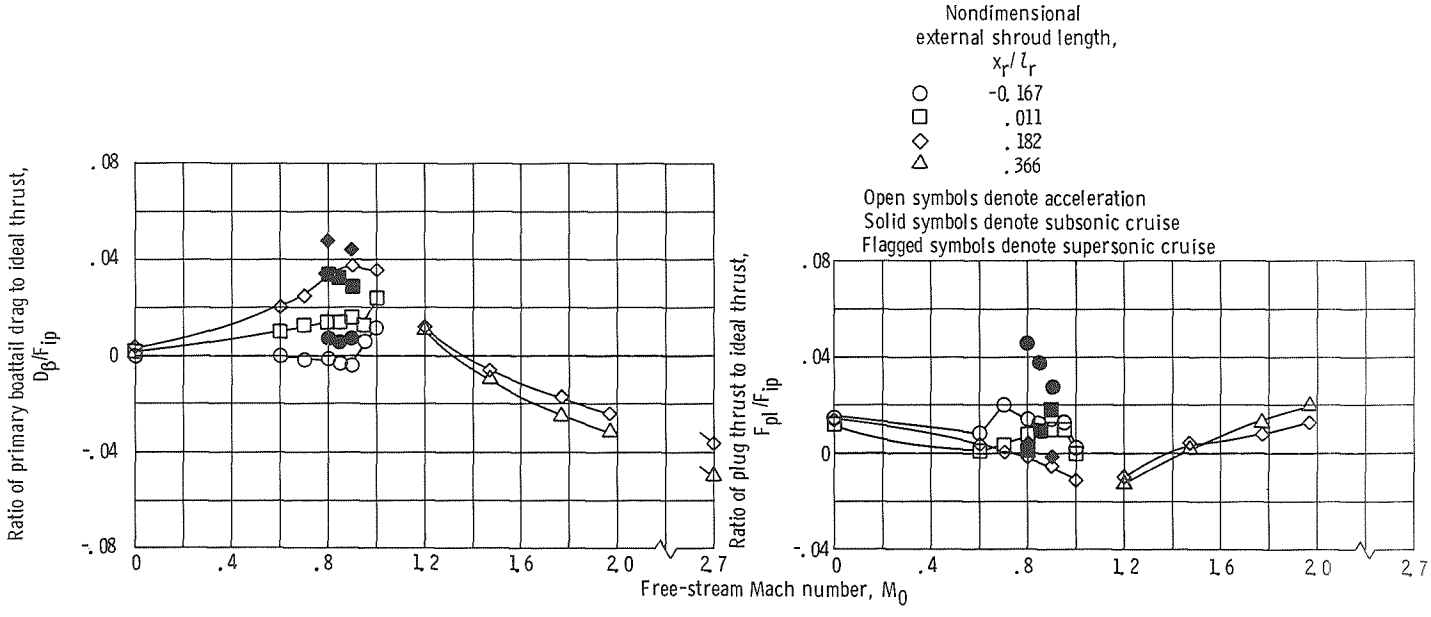

(c) Primary flap drag.

(d) Plug surface thrust.

Figure 10. - Concluded.

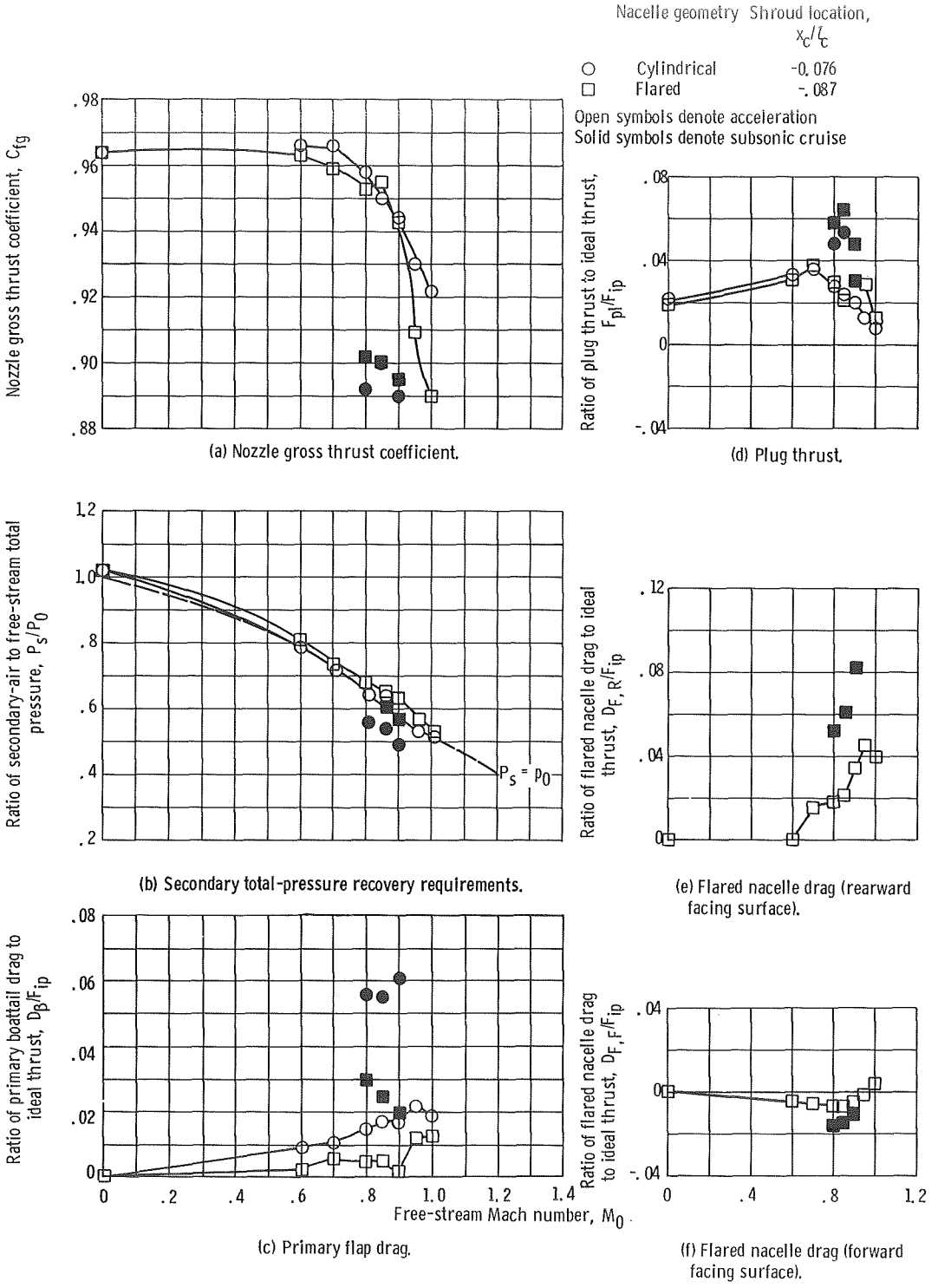

Figure 11. - Effect of nacelle geometry on nozzle performance characteristics. Full-length plug; 17° conical primary; corrected secondary weight flow ratio, $(w_s/w_p)\sqrt{T_s/T_p} = 0.04$.

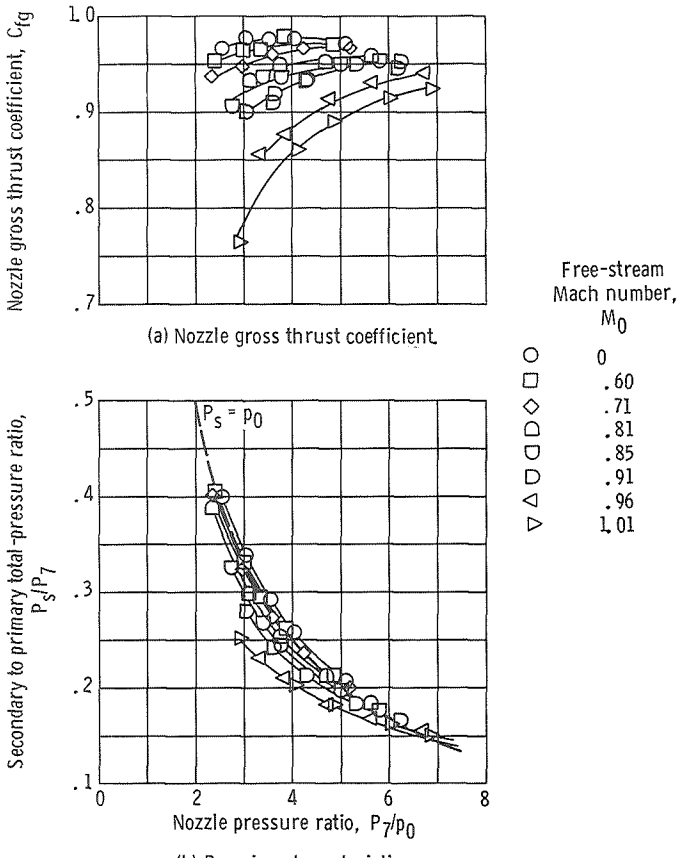

(a) Nozzle gross thrust coefficient.

(b) Pumping characteristics.

Figure 12. - Effect of nozzle pressure ratio on nozzle performance characteristics for full-length plug. Shroud location, $x_c/l_c = -0.116$; 17° conical primary; corrected secondary weight flow ratio, $(w_s/w_p)\sqrt{T_s/T_p} = 0.04$.

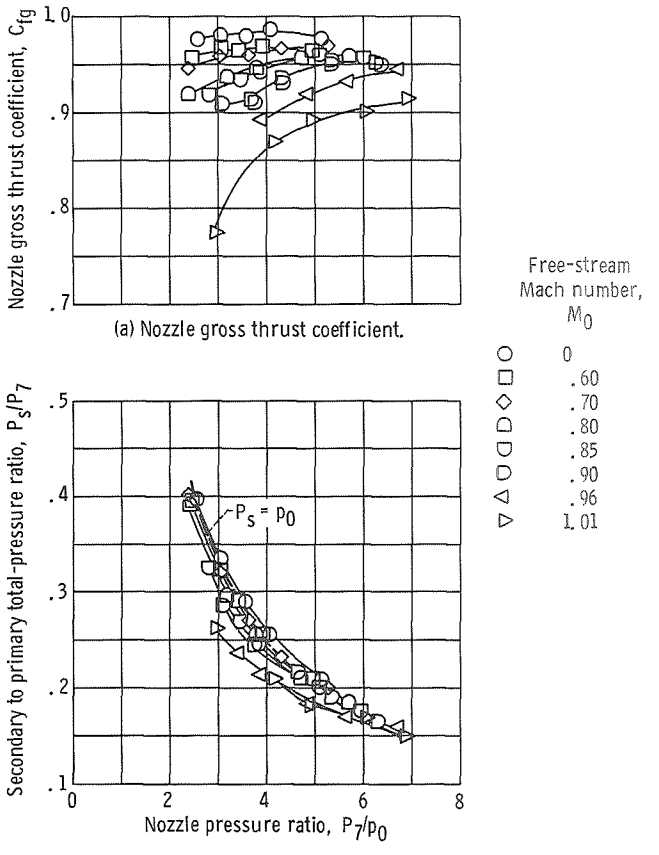

(a) Nozzle gross thrust coefficient.

(b) Pumping characteristics.

Figure 13. - Effect of nozzle pressure ratio on nozzle performance characteristics for 75-percent plug (open base). Shroud location, $x_c/l_c = -0.116$; 17° conical primary; corrected secondary weight flow ratio, $(w_s/w_p)\sqrt{T_s/T_p} = 0.04$.

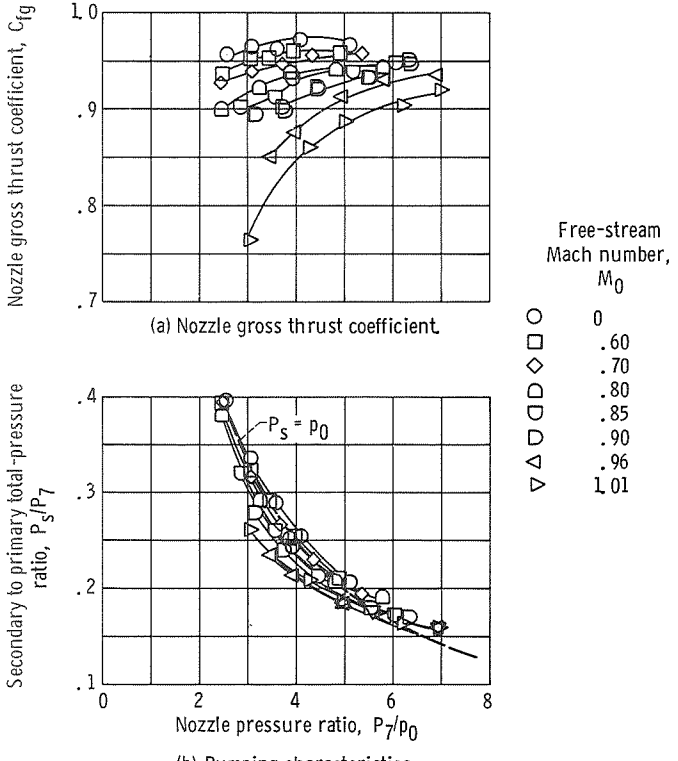

Figure 14. - Effect of nozzle pressure ratio on nozzle performance characteristics for 50-percent plug (open base). Shroud location, $x_c/l_c = -0.116$; 17° conical primary; corrected secondary weight flow ratio, $(w_s/w_p)\sqrt{T_s/T_p} = 0.04$.

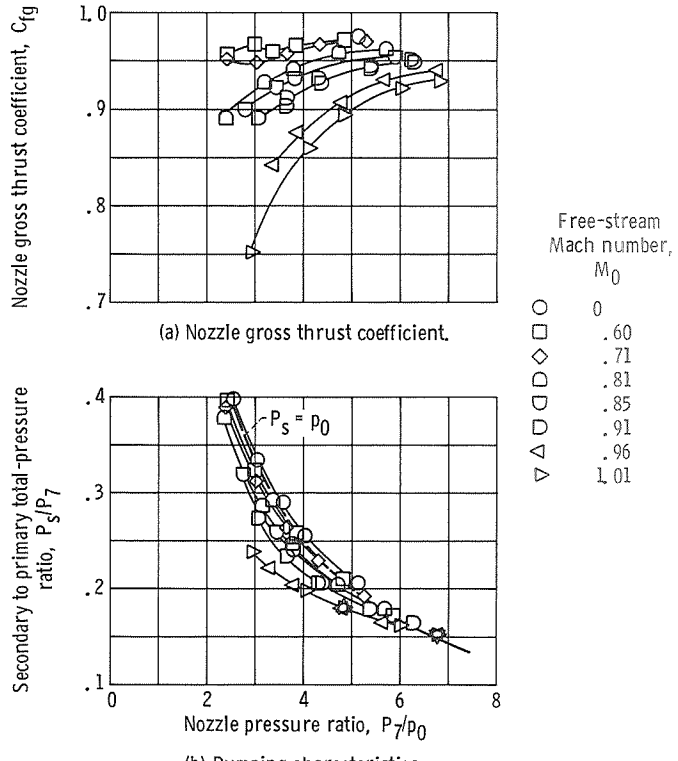

Figure 15. - Effect of nozzle pressure ratio on nozzle performance characteristics for shroud location (x_c/l_c) of -0.076. Full-length plug; 17° conical primary; corrected secondary weight flow ratio, $(w_s/w_p)\sqrt{T_s/T_p} = 0.04$.

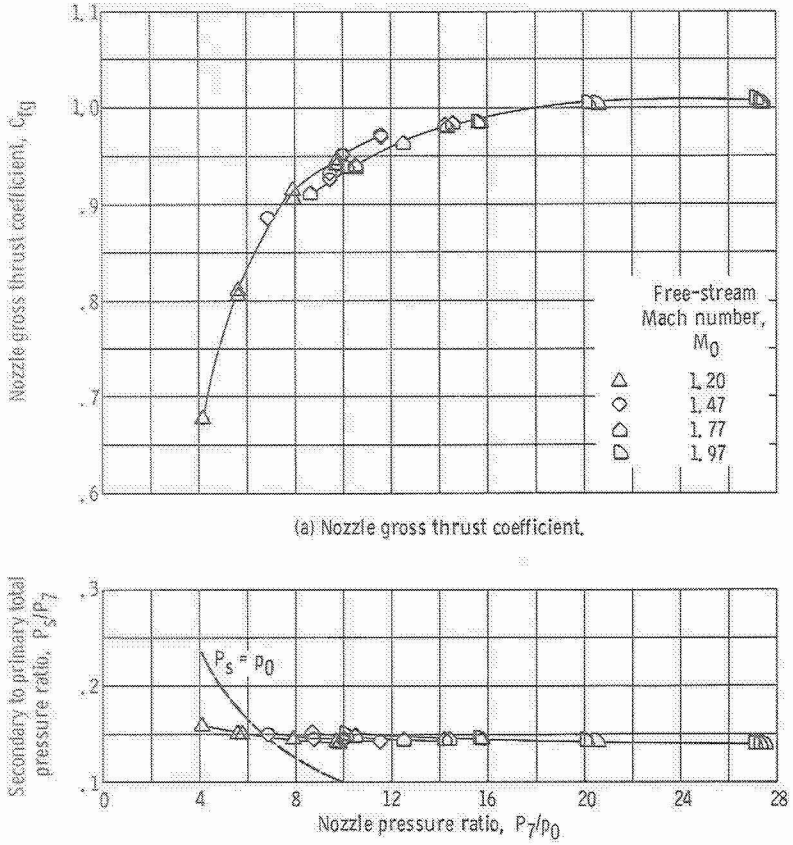

(a) Nozzle gross thrust coefficient.

(b) Pumping characteristics.

Figure 16. - Effect of nozzle pressure ratio on nozzle performance characteristics for shroud location (x_c/l_c) of 0.223. Full-length plug; 17° conical primary; corrected secondary weight flow ratio, $(w_s/w_p)\sqrt{T_s/T_p} = 0.04$.

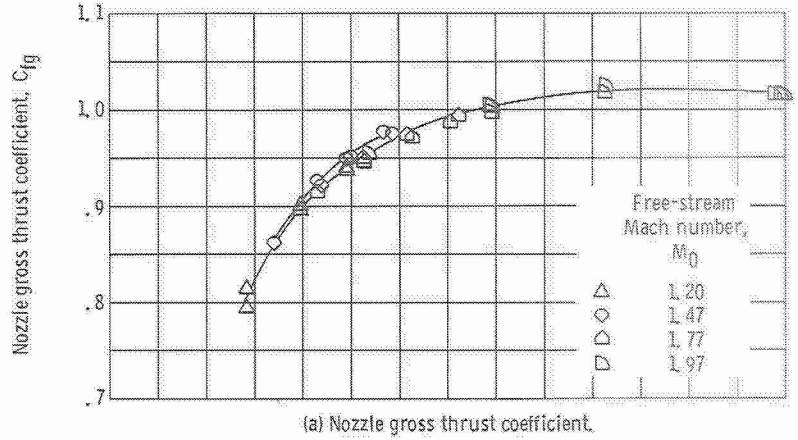

(a) Nozzle gross thrust coefficient.

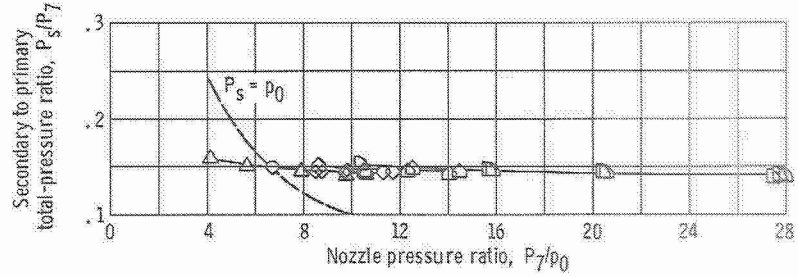

(b) Pumping characteristics.

Figure 17. - Effect of nozzle pressure ratio on nozzle performance characteristics for shroud location (x_c/l_c) of 0.347. Full-length plug; 17° conical primary; corrected secondary weight flow ratio, $(w_s/w_p)\sqrt{T_s/T_p} = 0.04$.

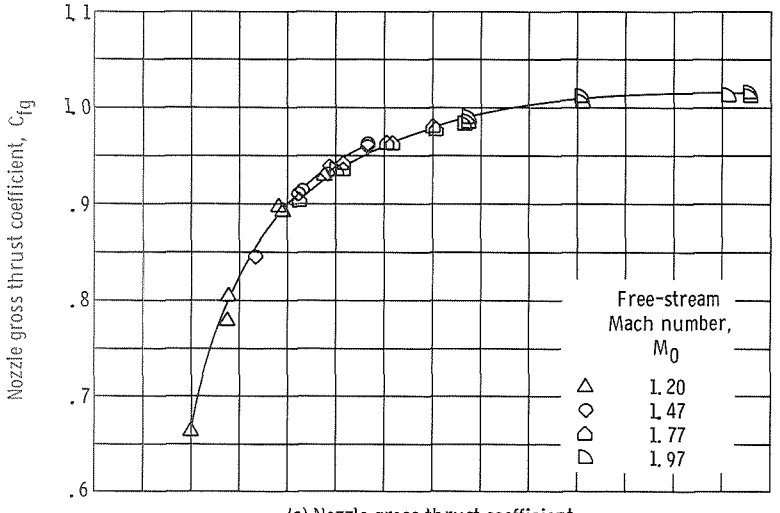

(a) Nozzle gross thrust coefficient.

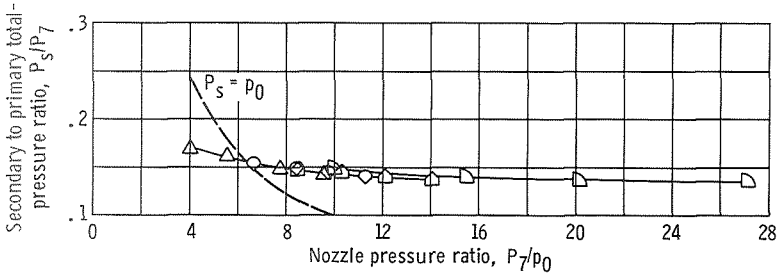

(b) Pumping characteristics.

Figure 18. - Effect of nozzle pressure ratio on nozzle performance characteristics for 75-percent plug (open base). Shroud location, $x_c/l_c = 0.347$; 17° conical primary; corrected secondary weight flow ratio, $(w_s/w_p)\sqrt{T_s/T_p} = 0.04$.

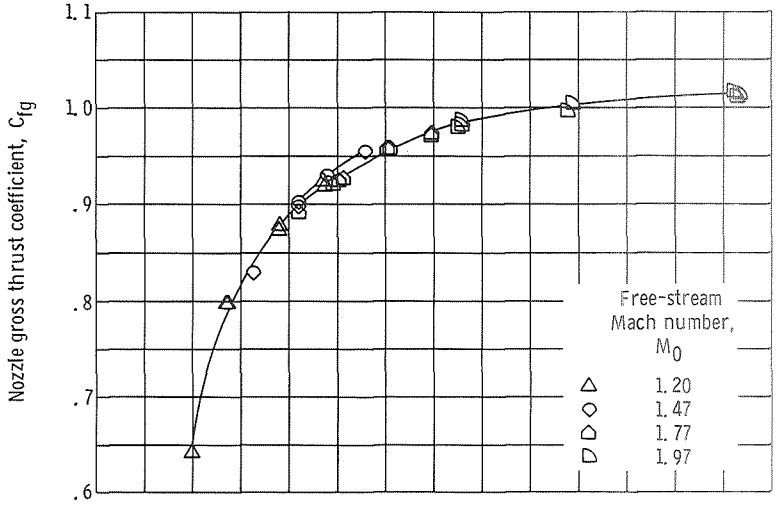

(a) Nozzle gross thrust coefficient.

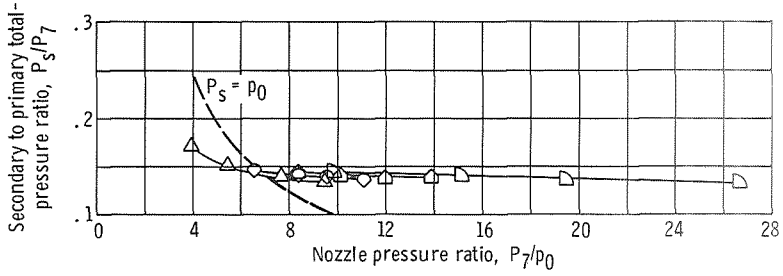

(b) Pumping characteristics.

Figure 19. - Effect of nozzle pressure ratio on nozzle performance characteristics for 50-percent plug (open base). Shroud location, $x_c/l_c = 0.347$; 17° conical primary; corrected secondary weight flow rate, $(w_s/w_p)\sqrt{T_s/T_p} = 0.04$.

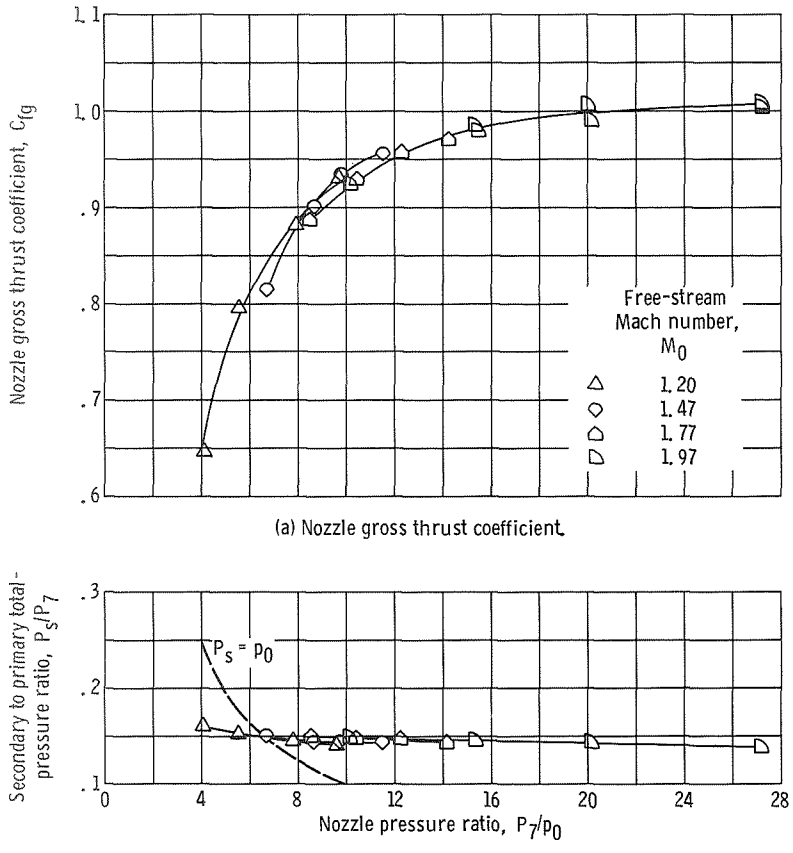

(a) Nozzle gross thrust coefficient.

(b) Pumping characteristics.

Figure 20. - Effect of nozzle pressure ratio on nozzle performance characteristics for 50-percent plug (closed base). Shroud location, $x_c/l_c = 0.347$; 17° conical primary; corrected secondary weight flow ratio, $(w_s/w_p)\sqrt{T_s/T_p} = 0.04$.

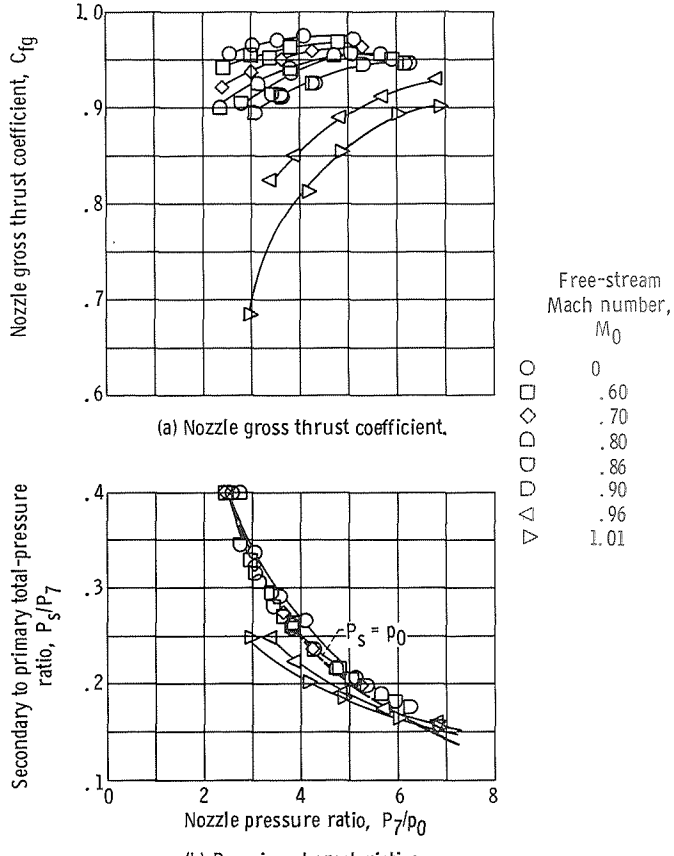

(a) Nozzle gross thrust coefficient.

(b) Pumping characteristics.

Figure 21. - Effect of nozzle pressure ratio on nozzle performance characteristics for shroud location (x_c/l_c) of -0.087. Full-length plug; flared nacelle; 17° conical primary; corrected secondary weight flow ratio, $(w_s/w_p)\sqrt{T_s/T_p} = 0.04$.

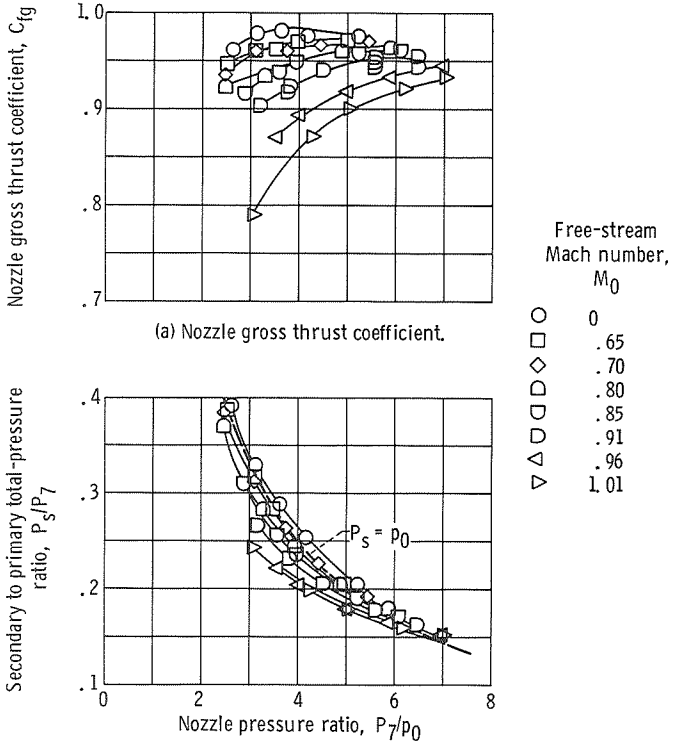

(a) Nozzle gross thrust coefficient.

(b) Pumping characteristics.

Figure 22. - Effect of nozzle pressure ratio on nozzle performance characteristics for shroud length (x_c/l_c) of -0.116. Full-length plug; 14° conical primary; corrected secondary weight flow ratio, $(w_s/w_p)\sqrt{T_s/T_p} = 0.04$.

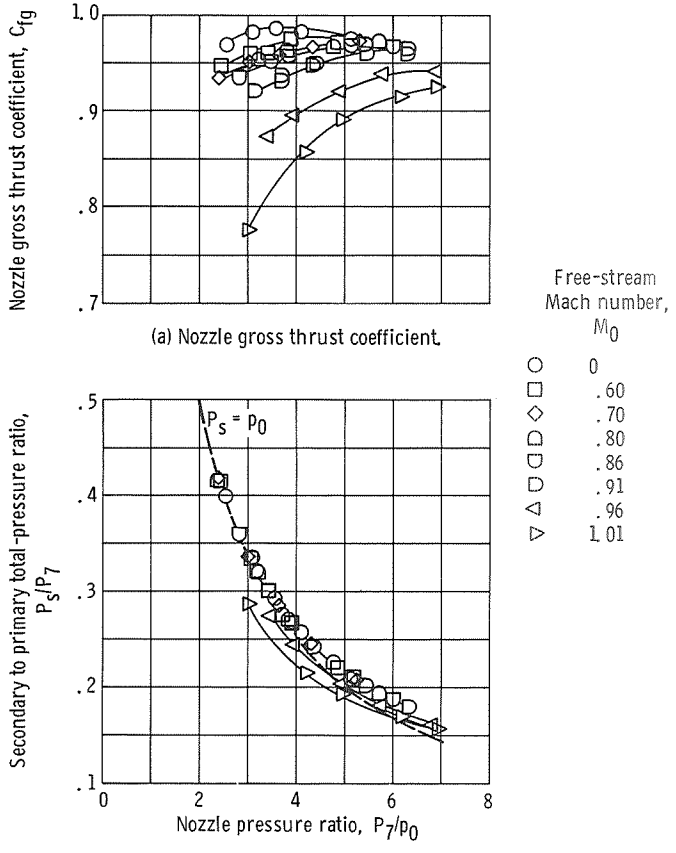

(a) Nozzle gross thrust coefficient.

(b) Pumping characteristics.

Figure 23. - Effect of nozzle pressure ratio on nozzle performance characteristics for shroud length (x_r/l_r) of -0.167. Full-length plug; 14° rounded primary; corrected secondary weight flow ratio, $(w_s/w_p)\sqrt{T_s/T_p} = 0.04$.

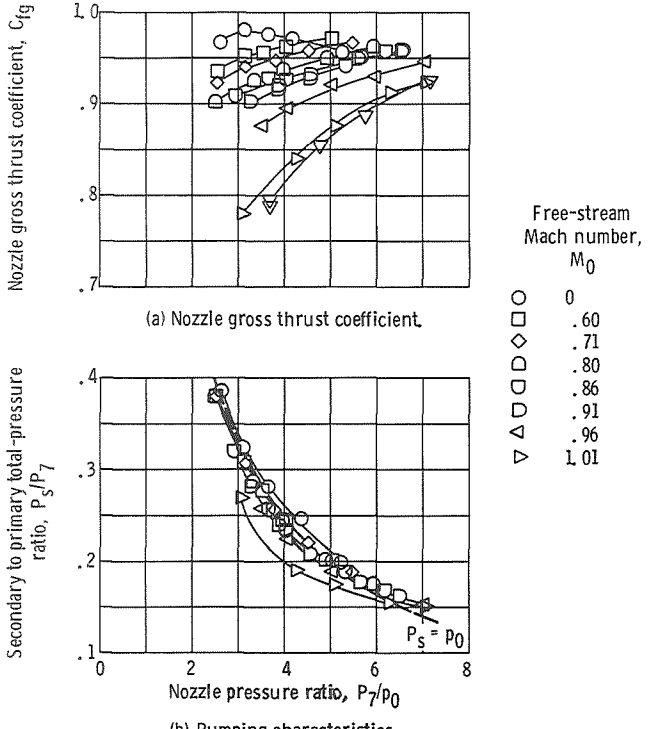

(a) Nozzle gross thrust coefficient.

(b) Pumping characteristics.

Figure 24. - Effect of nozzle pressure ratio on nozzle performance characteristics for shroud location (x_r/l_r) of 0.011. Full-length plug; 14° rounded primary; corrected secondary weight flow ratio, $(w_s/w_p)\sqrt{T_s/T_p} = 0.04$.

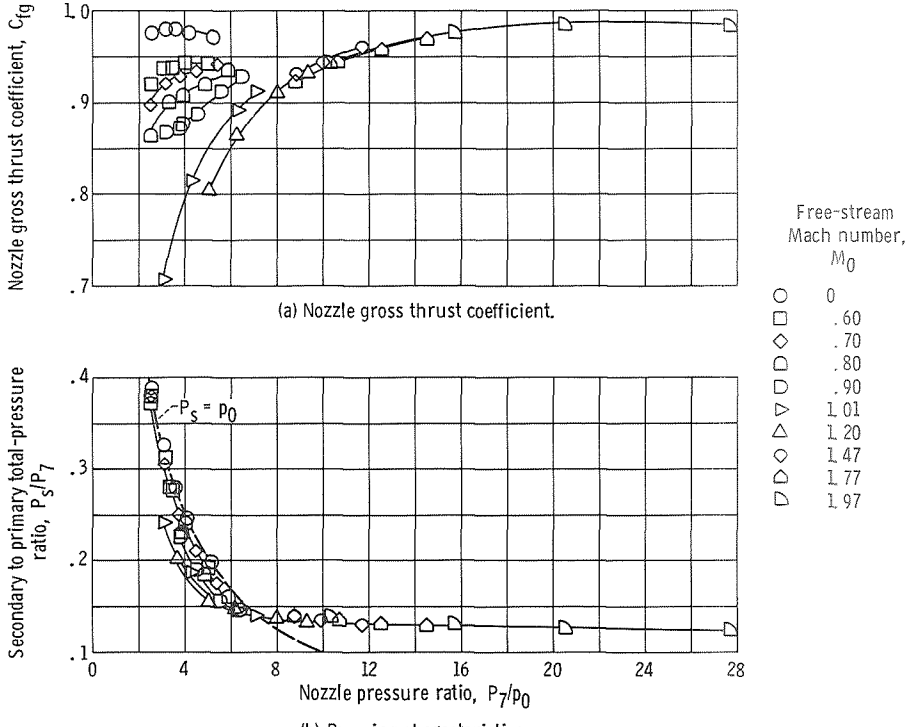

(a) Nozzle gross thrust coefficient.

(b) Pumping characteristics.

Figure 25. - Effect of nozzle pressure ratio on nozzle performance characteristics for shroud location (x_r/l_r) of 0.182. Full-length plug; 14° rounded primary; corrected secondary weight flow ratio, $(w_s/w_p)\sqrt{T_s/T_p} = 0.04$.

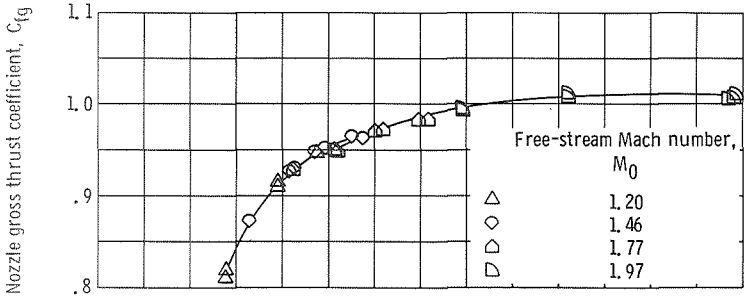

(a) Nozzle gross thrust coefficient.

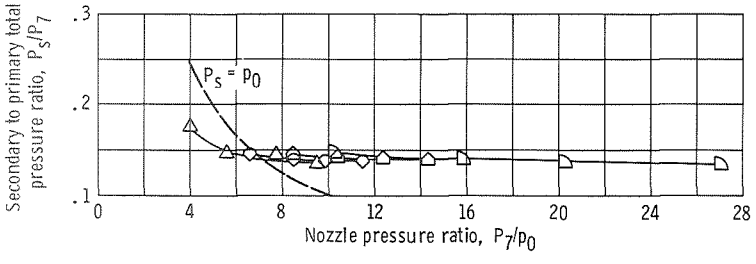

(b) Pumping characteristics.

Figure 26. - Effect of nozzle pressure ratio on nozzle performance characteristics for shroud location (x_r/l_r) of 0.366. Full-length plug; 14° rounded primary; corrected secondary weight flow ratio, $(w_s/w_p)\sqrt{T_s/T_p} = 0.04$.

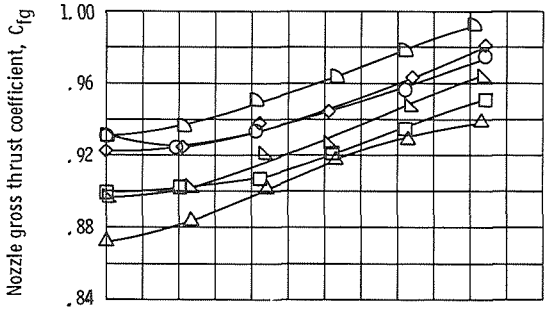

(a) Nozzle gross thrust coefficient.

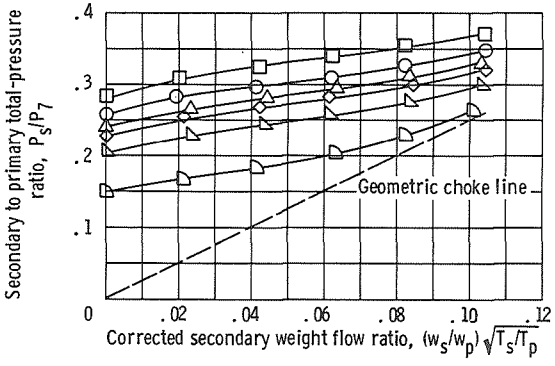

(b) Pumping characteristics.

	Free-stream Mach number, M_0	Nozzle pressure ratio, P_7/p_0
○	0.81	3.13
□	.85	2.73
◇	.85	3.40
△	.91	3.04
◿	.91	3.62
▱	.91	5.32

Figure 27. - Effect of corrected secondary weight flow ratio on nozzle performance characteristics for full-length plug. Shroud location, $x_c/l_c = -0.116$; 17° conical primary.

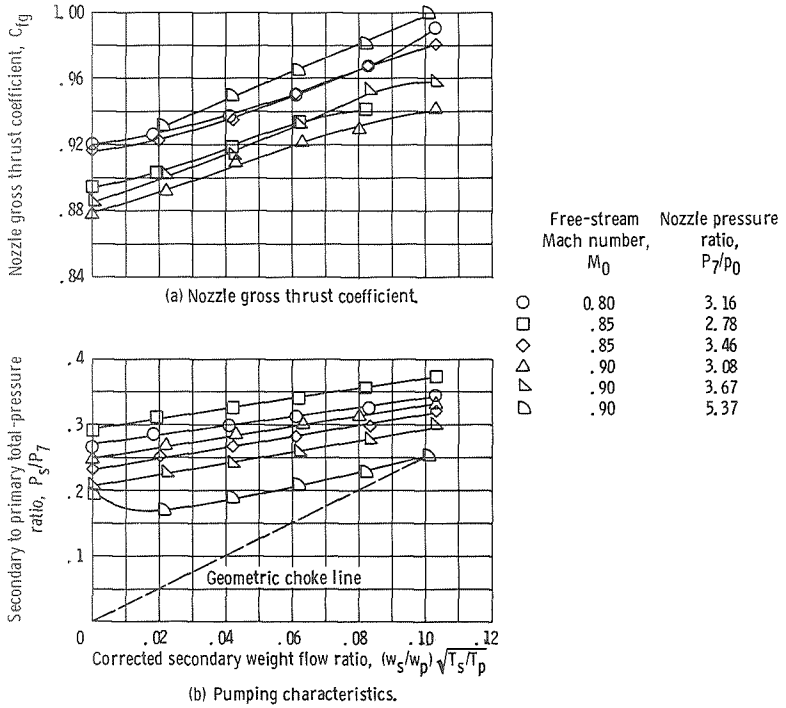

(a) Nozzle gross thrust coefficient.

(b) Pumping characteristics.

Figure 28. - Effect of corrected secondary weight flow ratio on nozzle performance characteristics for 75-percent plug (open base). Shroud location, x_c/l_c = -0.116; 17° conical primary.

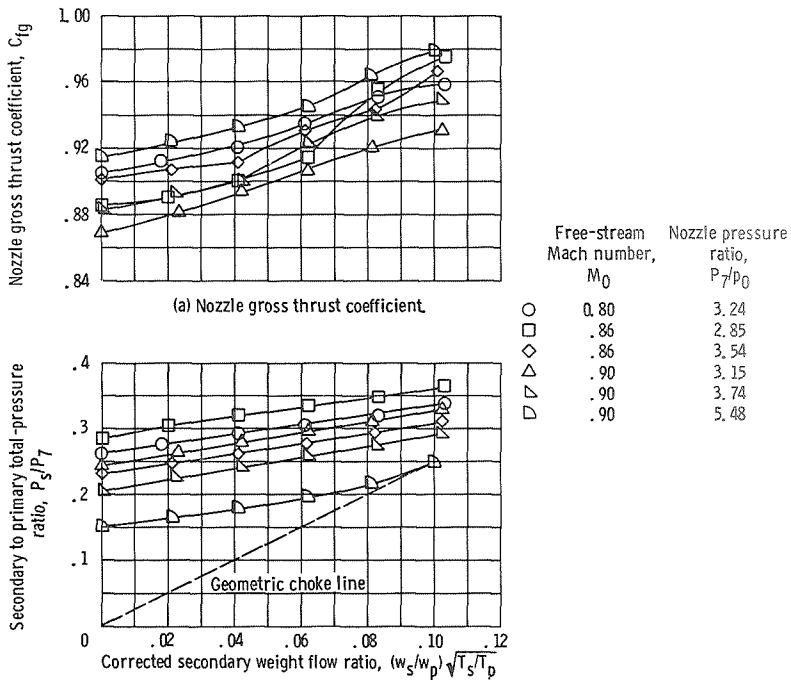

(a) Nozzle gross thrust coefficient.

(b) Pumping characteristics.

Figure 29. - Effect of corrected secondary weight flow ratio on nozzle performance characteristics for 50-percent plug (open base). Shroud location, x_c/l_c = -0.116; 17° conical primary.

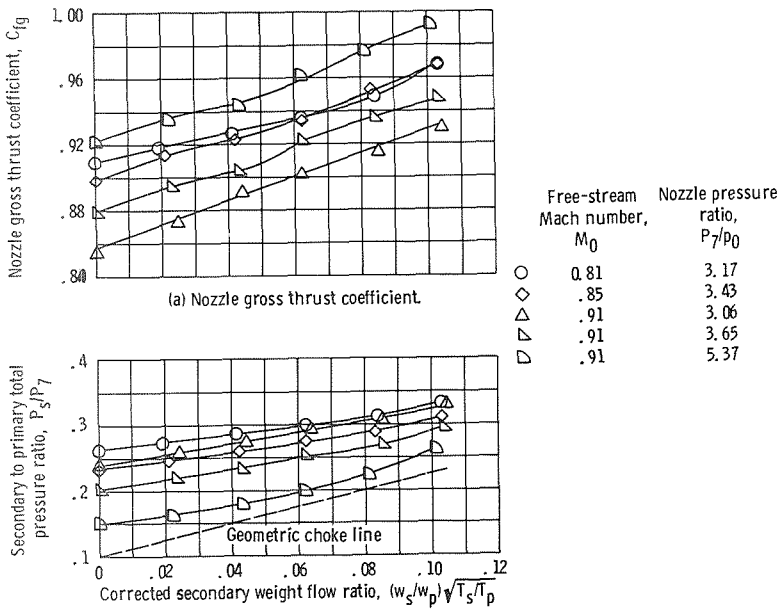

(a) Nozzle gross thrust coefficient.

(b) Pumping characteristics.

Figure 30. - Effect of corrected secondary weight flow ratio on nozzle performance characteristics for shroud location (x_c/l_c) of -0.076. Full-length plug; 17° conical primary.

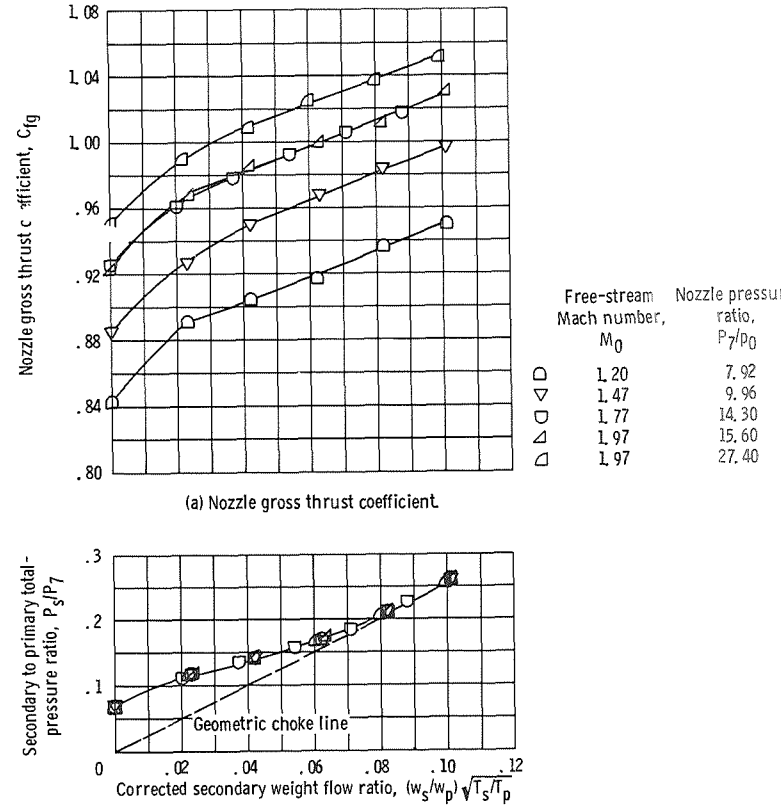

(a) Nozzle gross thrust coefficient.

(b) Pumping characteristics.

Figure 31. - Effect of corrected secondary weight flow ratio on nozzle performance characteristics for shroud location (x_c/l_c) of 0.223. Full-length plug; 17° conical primary.

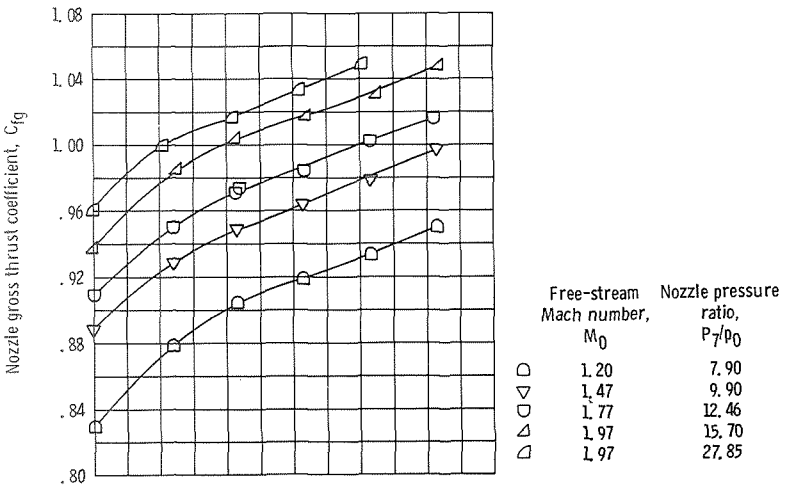

(a) Nozzle gross thrust coefficient.

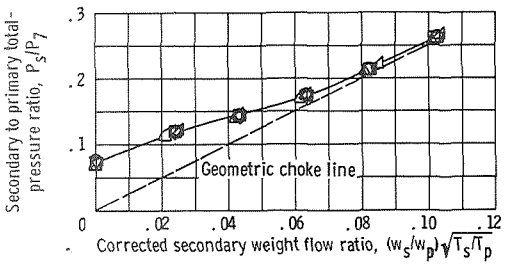

(b) Pumping characteristics.

Figure 32. - Effect of corrected secondary weight flow ratio on nozzle performance characteristics for shroud location (x_c/l_c) of 0.347. Full-length plug; 17° conical primary.

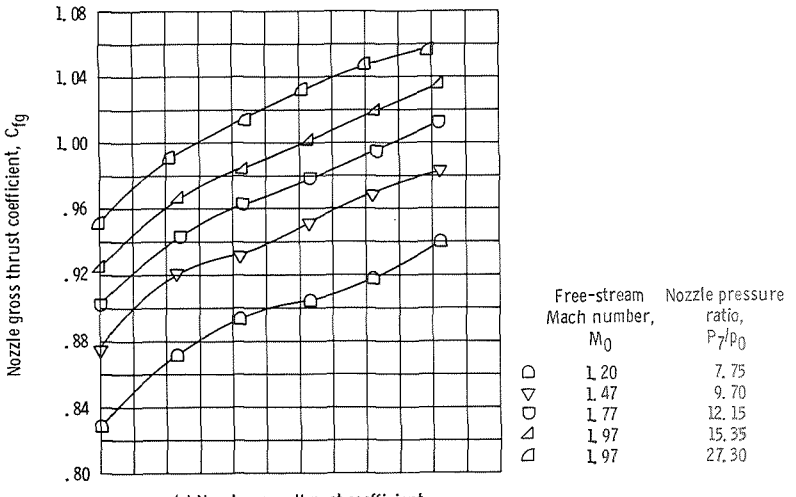

(a) Nozzle gross thrust coefficient.

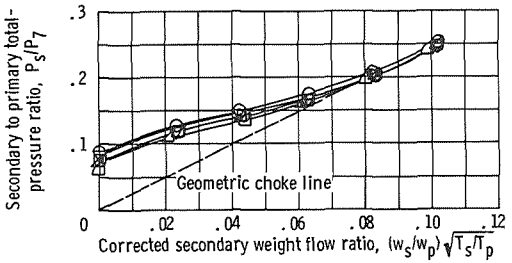

(b) Pumping characteristics.

Figure 33. - Effect of corrected secondary weight flow ratio on nozzle performance characteristics for 75-percent plug (open base). Shroud location, x_c/l_c = 0.347; 17° conical primary.

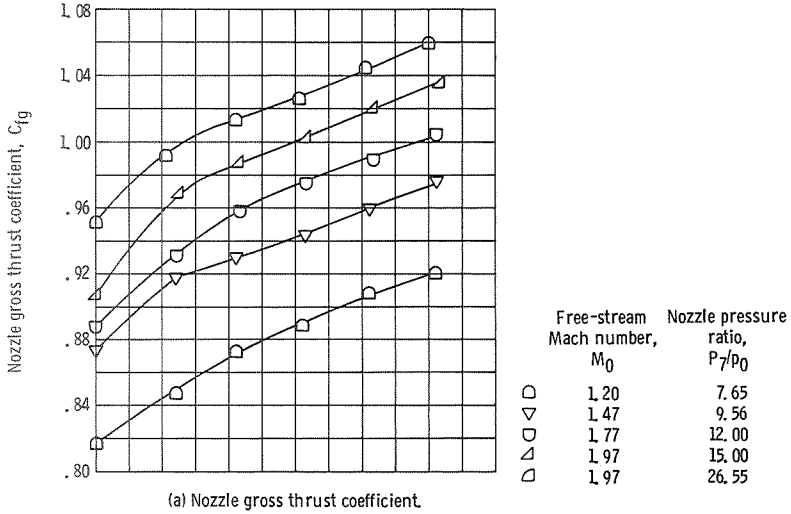

(a) Nozzle gross thrust coefficient.

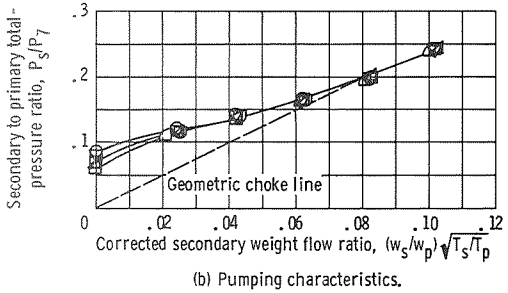

(b) Pumping characteristics.

Figure 34. - Effect of corrected secondary weight flow ratio on nozzle performance characteristics for 50-percent plug (open base). Shroud location, x_c/l_c = 0.347; 17° conical primary.

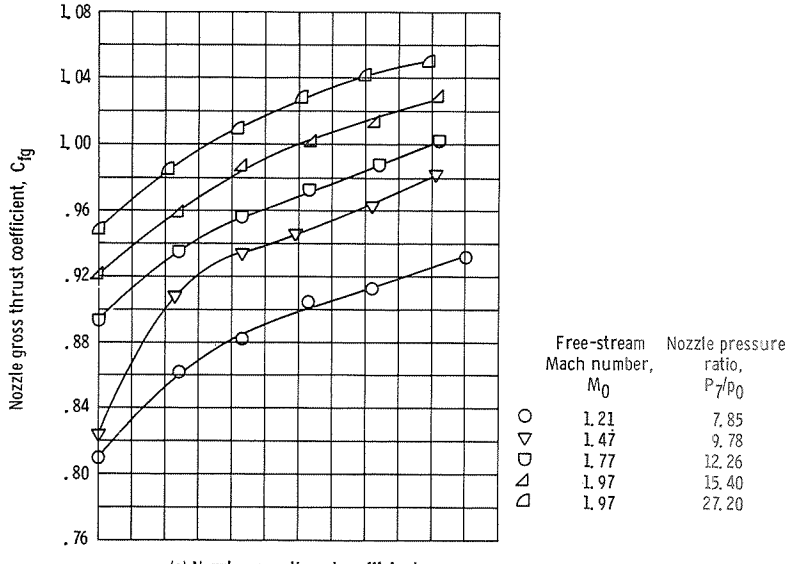

(a) Nozzle gross thrust coefficient.

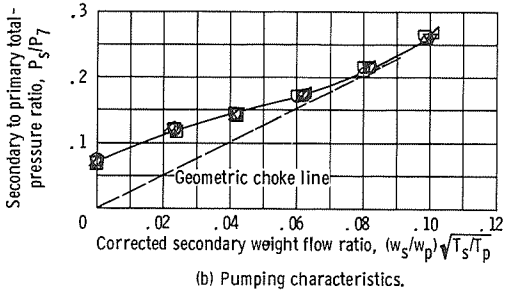

(b) Pumping characteristics.

Figure 35. - Effect of corrected secondary weight flow ratio on nozzle performance characteristics for 50-percent plug (closed base). Shroud location, x_c/l_c = 0.347; 17° conical primary.

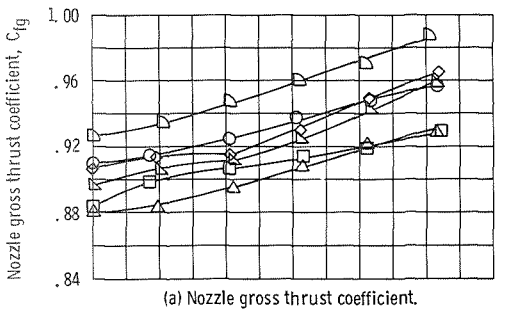

(a) Nozzle gross thrust coefficient.

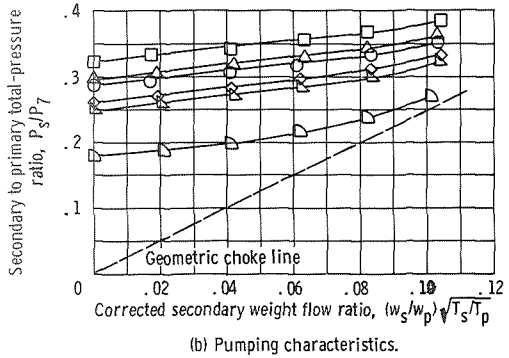

(b) Pumping characteristics.

	Free-stream Mach number, M_0	Nozzle pressure ratio, P_7/p_0
○	0.80	3.16
□	.86	2.78
◇	.86	3.45
△	.90	3.05
◁	.90	3.64
▱	.90	5.34

Figure 36. - Effect of corrected secondary weight flow ratio on nozzle performance characteristics for shroud location (x_c/l_c) of -0.087. Full-length plug; flared nacelle; 17° conical primary.

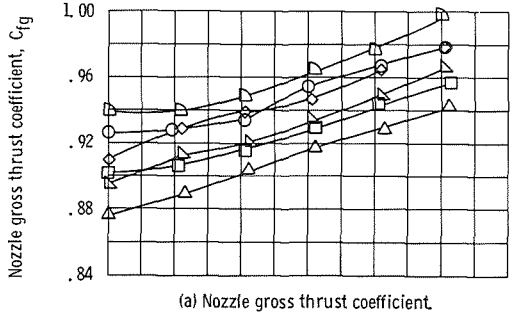

(a) Nozzle gross thrust coefficient.

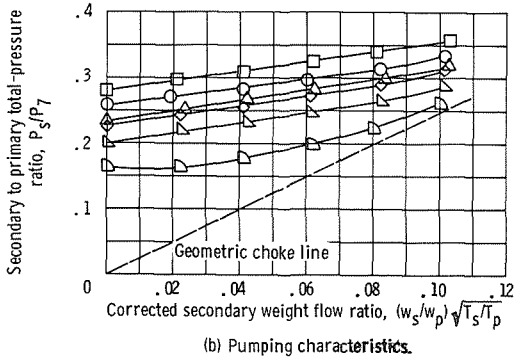

(b) Pumping characteristics.

	Free-stream Mach number, M_0	Nozzle pressure ratio, P_7/p_0
○	0.80	3.29
□	.85	2.86
◇	.85	3.56
△	.91	3.19
◁	.91	3.79
▱	.91	5.55

Figure 37. - Effect of corrected secondary weight flow ratio on nozzle performance characteristics for shroud location (x_c/l_c) of -0.116. Full-length plug; 14° conical primary.

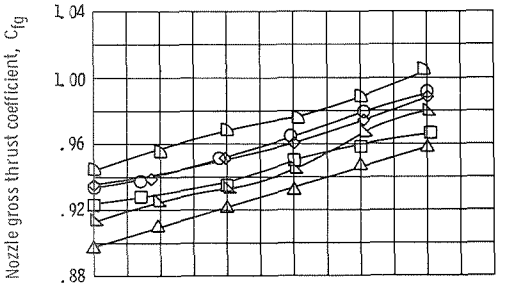

(a) Nozzle gross thrust coefficient.

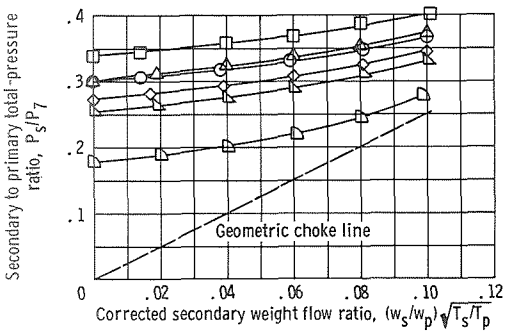

(b) Pumping characteristics.

	Free-stream Mach number, M_0	Nozzle pressure ratio, P_7/p_0
○	0.80	3.20
□	.86	2.81
◇	.86	3.49
△	.91	3.12
◁	.91	3.70
▱	.91	5.43

Figure 38. - Effect of corrected secondary weight flow ratio on nozzle performance characteristics for shroud location (x_r/l_r) of -0.167. Full-length plug; 14° rounded primary.

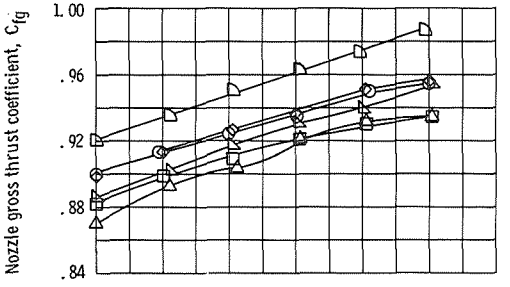

(a) Nozzle gross thrust coefficient.

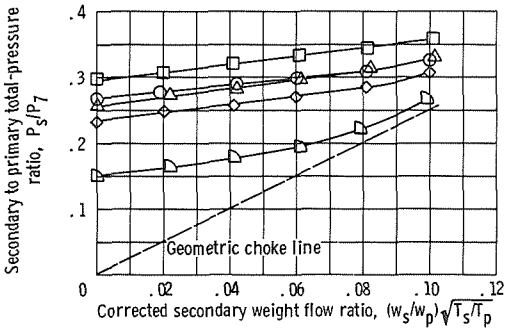

(b) Pumping characteristics.

	Free-stream Mach number, M_0	Nozzle pressure ratio, P_7/p_0
○	0.80	3.30
□	.86	2.92
◇	.86	3.63
△	.91	3.25
◁	.91	3.85
▱	.91	5.65

Figure 39. - Effect of corrected secondary weight flow ratio on nozzle performance characteristics for shroud location (x_r/l_r) of 0.011. Full-length plug; 14° rounded primary.

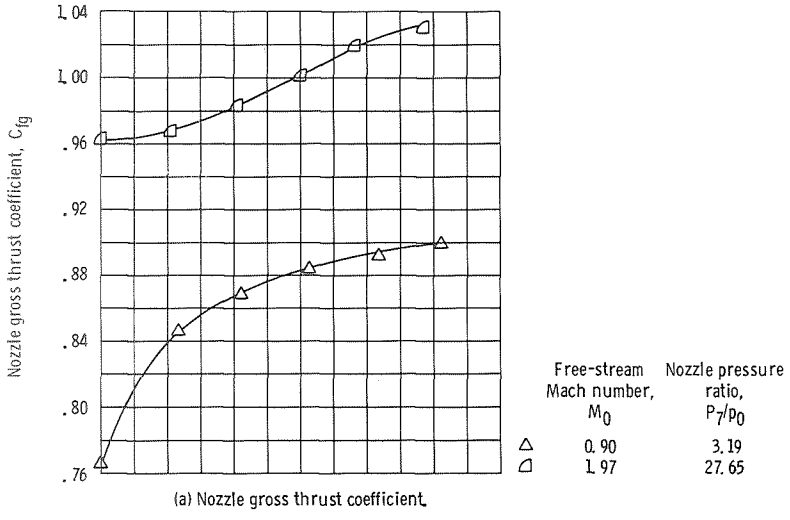

(a) Nozzle gross thrust coefficient.

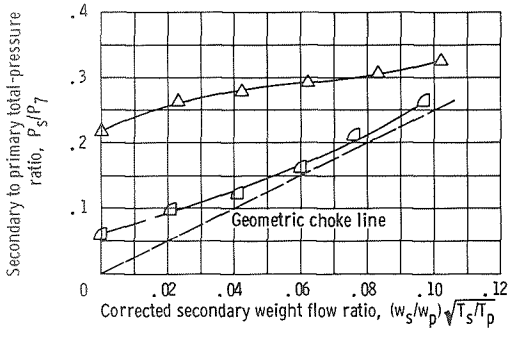

(b) Pumping characteristics.

Figure 40. - Effect of corrected secondary weight flow ratio on nozzle performance characteristics for shroud location (x_r/l_r) of 0.182. Full-length plug; 14° rounded primary.

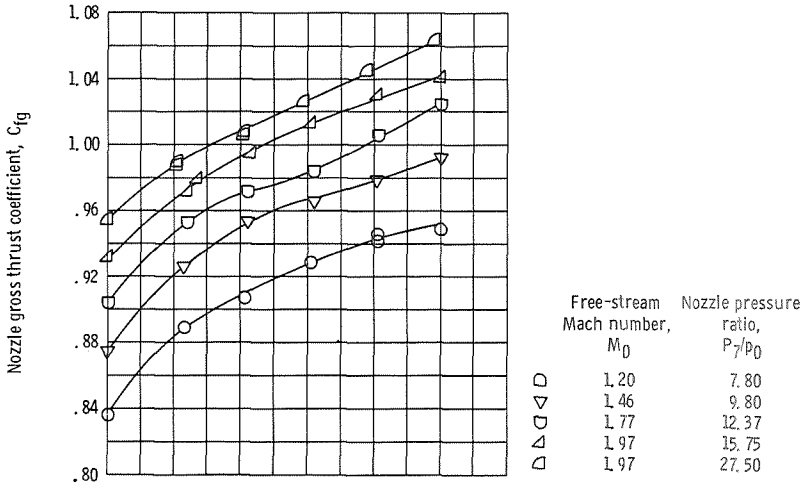

(a) Nozzle gross thrust coefficient.

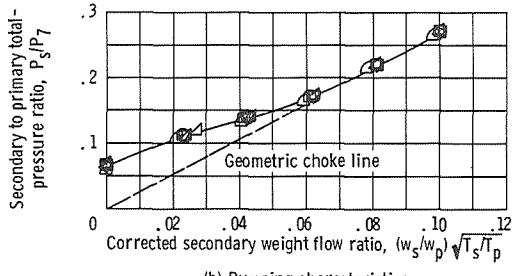

(b) Pumping characteristics.

Figure 41. - Effect of corrected secondary weight flow ratio on nozzle performance characteristics for shroud location (x_r/l_r) of 0.366. Full-length plug; 14° rounded primary.

"The aeronautical and space activities of the United States shall be conducted so as to contribute . . . to the expansion of human knowledge of phenomena in the atmosphere and space. The Administration shall provide for the widest practicable and appropriate dissemination of information concerning its activities and the results thereof."

—NATIONAL AERONAUTICS AND SPACE ACT OF 1958

NASA SCIENTIFIC AND TECHNICAL PUBLICATIONS

TECHNICAL REPORTS: Scientific and technical information considered important, complete, and a lasting contribution to existing knowledge.

TECHNICAL NOTES: Information less broad in scope but nevertheless of importance as a contribution to existing knowledge.

TECHNICAL MEMORANDUMS: Information receiving limited distribution because of preliminary data, security classification, or other reasons.

CONTRACTOR REPORTS: Scientific and technical information generated under a NASA contract or grant and considered an important contribution to existing knowledge.

TECHNICAL TRANSLATIONS: Information published in a foreign language considered to merit NASA distribution in English.

SPECIAL PUBLICATIONS: Information derived from or of value to NASA activities. Publications include conference proceedings, monographs, data compilations, handbooks, sourcebooks, and special bibliographies.

TECHNOLOGY UTILIZATION PUBLICATIONS: Information on technology used by NASA that may be of particular interest in commercial and other non-aerospace applications. Publications include Tech Briefs, Technology Utilization Reports and Notes, and Technology Surveys.

Details on the availability of these publications may be obtained from:

SCIENTIFIC AND TECHNICAL INFORMATION DIVISION
NATIONAL AERONAUTICS AND SPACE ADMINISTRATION
Washington, D.C. 20546